63-3-5

THIRD QUARTERLY PROGRESS REPORT ON ADVANCED ANTENNA DESIGN TECHNIQUES

16 DECEMBER 1962 THROUGH 28 FEBRUARY 1963

GER 11045
Report No. 3

28 March 1963
Copy No. _____

Contract DA-36-039 SC-90746

DA Project No. 3A99-12-001

U. S. Army Electronics Research and Development Laboratory
Fort Monmouth, New Jersey

GOODYEAR AIRCRAFT CORPORATION
AKRON 15, OHIO

THIRD QUARTERLY PROGRESS REPORT ON ADVANCED ANTENNA DESIGN TECHNIQUES

16 DECEMBER 1962 THROUGH 28 FEBRUARY 1963

GER 11045
Report No. 3

28 March 1963
Copy No. ____

Prepared by

D. D. Collins and J. C. Bell Jr.

Contract DA-36-039 SC-90746

Signal Corps Technical Requirements No. SCL-4346
dated 23 October 1961, as amended by Contract
Article I - Statement of Work dated 31 May 1962

DA Project No. 3A99-12-001

U. S. Army Electronics Research and Development Laboratory
Fort Monmouth, New Jersey

GOODYEAR AIRCRAFT CORPORATION
AKRON 15, OHIO

Objective: To assess the particular needs of two broad categories of application (1) space vehicle antennas and (2) ground-based tracking antennas, and to conduct design studies leading to the generation of new concepts, materials, techniques, and practical designs for lightweight and economical antenna systems. To demonstrate the feasibility of the three most promising concepts with suitable models.

TABLE OF CONTENTS

TABLE OF CONTENTS (Continued)

LIST OF ILLUSTRATIONS

LIST OF ILLUSTRATIONS (Continued)

LIST OF TABLES

PART 1 - PURPOSE

The purposes of this contract are to assess the particular needs of two broad categories of antenna applications: (1) space vehicle (satellite) antenna systems and (2) ground-based tracking antennas including radomes and to conduct design studies leading to the generation of new concepts, materials, techniques, and practical designs for lightweight and economical antenna systems. These studies will lead to the design and fabrication of models for the three most promising concepts, which will be utilized to demonstrate feasibility of these concepts.

For space vehicle antenna systems, the goal is to develop concepts and practical designs for large aperture appendage arrays and discrete radiators which will provide the best stowage to final dimension ratio, lowest possible weight, and lowest cost.

For ground-based tracking antennas, the goal is to develop concepts and practical designs for large aperture collimators, large arrays, and sub-array elements of minimum weight and low cost which can be simply and economically assembled and erected on site.

This program effort has been broken down into six discrete phases as follows:

Phase I - System Parameter Investigation

This phase established the system parameters for antenna designs consistent with the specified requirements. Specifically, this phase established the size of the antennas to be studied as well as the power requirements, the environmental conditions, and the structural design parameters.

Phase II - Concept Generation and Preliminary Evaluation

During this phase, various antenna system concepts were generated and given a preliminary evaluation. The concepts that appeared most desirable from the standpoint of meeting the established requirements and economy were selected for further study. This phase essentially represented the most creative part of the program. Many concepts were considered which include completely new approaches to the problem as well as new advances to the present state-of-the-art.

Phase III - Preliminary Analysis and Concept Selection

During this phase, the concepts selected for further study in Phase II were given a preliminary analysis. Based on this analysis and a comparison of economy of each, the space and ground concepts were further weeded out until two or three of the most promising of each remained. From these concepts, three were selected for detail design study and analysis.

Phase IV - Detail Study and Analysis

During this phase, a more detail analysis of the remaining concepts will be made and will include performance and accuracy aspects, economy comparison with conventional antenna systems, and detail design and fabrication considerations.

Phase V - Models

During this phase, models of the three most promising antenna systems will be designed, fabricated, and tested. These models need not be complete models of the antenna systems, but will be laboratory-type models of the portions of the antenna systems needed to adequately demonstrate the feasibility of all unique or advanced state-of-the-art techniques or concepts employed.

Phase VI - Reports

The reporting phase will be concurrent with Phases I through V and includes 10 monthly letter-type reports, three formal quarterly reports, and one formal final report as required by the contract.

Figure 1 shows the work program broken down into phases and shows the time span allotted to each.

The following programs related to the objectives of this contract are under way at Goodyear Aircraft Corporation (GAC):

(1) GAC-supported development program to evaluate foams and their application techniques in conjunction with process improvement for utilization of foams for producing antenna reflector surfaces. Strength, dimensional stability, and durability required for antenna reflector surfaces are being considered.

(2) GAC-supported process development program to perfect and evaluate a technique for producing very accurate contoured antenna reflector surface by applying exothermic plastic material in thin layers over a rough reflector surface, utilizing a precision tool sweep method. The final reflective surface will be obtained by metal spraying or application of reflective paint to the hardened plastic surface.

(3) U.S. Air Force - RADC Contract AF30(602)2753 Pseudo-hardened Emergency Antenna Installation - Study Program. The purpose of this study program was to determine the feasibility of an air-supported, integrated radome - antenna configuration wherein a portion of the surface of the air-supported radome serves as the antenna reflector requiring rotation of only the feed system for scanning operation. This program involved design, fabrication, and antenna pattern testing of a scale model and development of design data for a full-scale concept.

PART 1 - PURPOSE

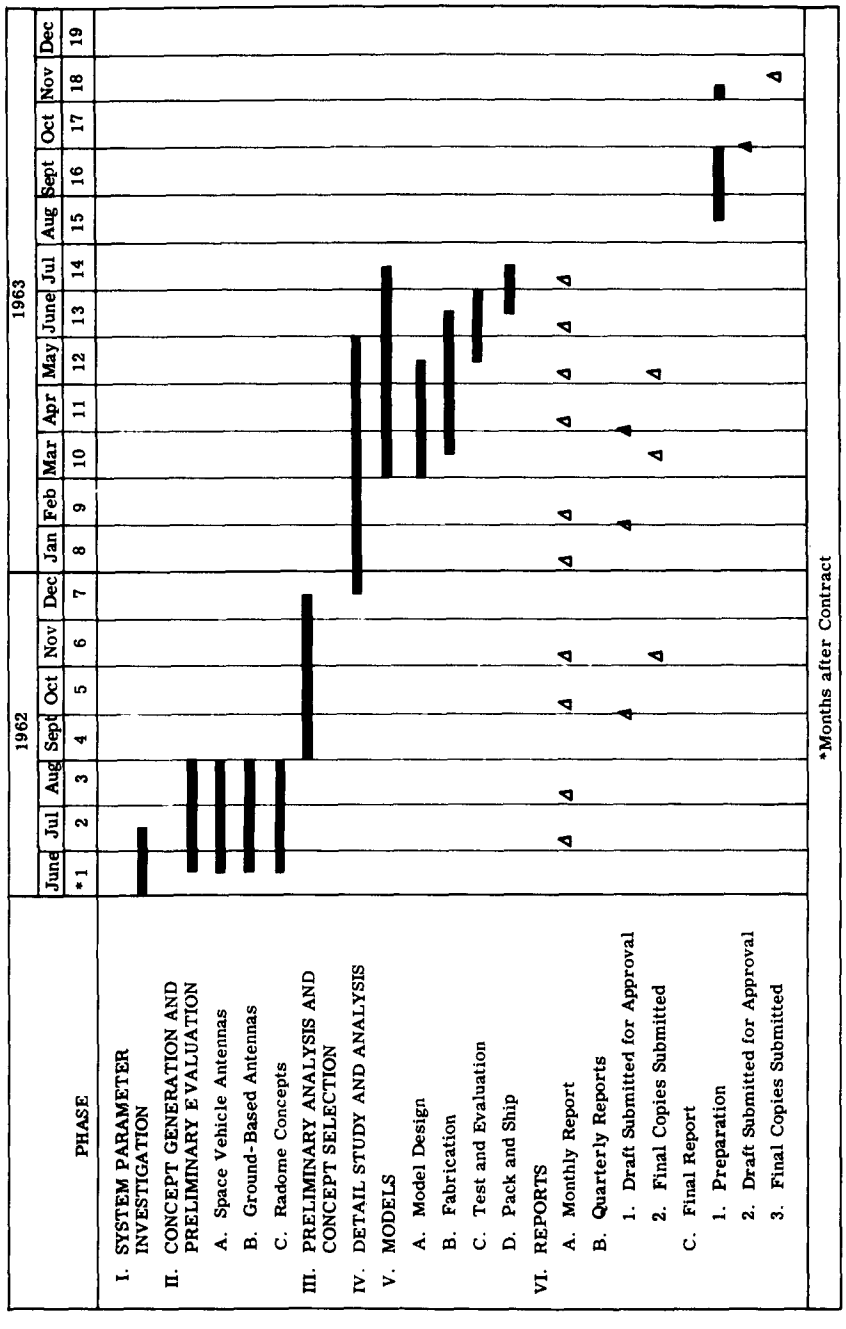

Figure 1 - Work Program for Advanced Antenna Design Study Program

(4) Contract with Airborne Instruments Laboratory to manufacture and erect two 17-foot-diameter polyurethane foam radomes for use with airport ground control radar equipment.

(5) GAC-supported general design and application study program to prove feasibility and establish general design criteria for microwave structures and antennas for space applications. The study will be supported with feasibility models and testing of materials, structures, rigidization techniques, and electrical characteristics.

(6) Subcontract with Sundstrand Corporation to design and produce an experimental preprototype 44.5-foot-diameter solar collector for USAF Prime Contract AF33(616)-7128. The object of this program is to design and produce an inflatable foam-rigidized parabolic solar concentrator of flight prototype size. The preprototype model is intended for optical evaluation and testing under ground environmental conditions; however, the design approach will be such as to permit early development to meet space application requirements.

(7) U.S. Air Force - ASD Contract AF33(657)-10165 Solar Reflector Foaming Technology Program. A study and investigation of the technology for foaming solar reflectors in space environment.

(8) GAC-supported theoretical study program to develop new design criteria for very high performance reflector antennas. The objectives of this program are to establish detail design criteria for optimum feed illumination for minimum achievable side lobes, blockage effects, and interrelation of these with tolerances.

PART 2 - ABSTRACT

This third quarterly report for the advanced antenna design program covers the initial part of Phase IV, detail study and analysis, and the initial detail design effort for Phase V, model design and fabrication. Here the rigid-panel Swirlabola* space vehicle antenna, the AIRMAT** paraboloid ground-based antenna, and the lenticular AIRMAT ground-based antenna, selected as having the best potential during Phase III of the program, are studied and analyzed in further detail. Detail design configurations for models of these three antennas are established.

General design goals and requirements are established for the rigid-panel Swirlabola space vehicle antenna. Electrical, structural, and mechanical design considerations are discussed. An aperture diameter of 10 feet and an f/D ratio of 0.35 are established. A contour accuracy of ± 1/24 inch is established as the upper design goal. Thermal and dynamic analyses are shown and indicate that thermal and dynamic deflections can be maintained within the required range. A scale model size of 3 feet in diameter has been established. Model design configuration is presented.

Electrical design considerations for the AIRMAT paraboloid ground-based antenna are discussed. The design is based on a 40-foot-diameter Cassegrain feed antenna with an f/D ratio of 0.35 for operation in the 10-kmc range. A

* A parabolic antenna reflector having petal-like reflector elements that unfold in a "swirl" fashion to form the parabolic reflector shape.

**TM, Goodyear Aircraft Corporation, Akron 15, Ohio

hyperbolic secondary reflector, 1.6 feet in diameter, is selected on a basis of minimum blockage and realistic feed horn design. The effects of the secondary reflector blockage on side lobe level are investigated, and no significant problems are indicated. A structural and deflection analysis is presented for this antenna, wherein inertial and antisymmetrical gravitational loadings are considered and show that the deflection can be maintained within required limits. The required drop cord and cover ply wire sizes are determined on a basis of allowable tip deflection. A mechanical design is presented for a maximum gain (minimum blockage) configuration.

Electrical design considerations for the lenticular AIRMAT ground-based antenna are discussed. The design is based on a 40-foot-diameter Cassegrain feed antenna with an f/D ratio of 0.35. In this case, a larger secondary reflector, 3.3 feet in diameter, is selected to permit location of the feed within the hub and improve the over-all packageability, with only minor performance degradation due to blockage. Here again, the effects of feed blockage on side lobe level are investigated. The phase delay of the energy propagated through the drop cords located between the primary and secondary reflectors is investigated. Calculations based on initial assumptions indicate that the use of this antenna may be limited to frequencies below approximately 5000 mc, due to the effects of the drop cords. A preliminary structural analysis based on a symmetrical gravitational loading is presented. Results show that, for this condition, deflections are well within required limits. A mechanical design configuration is presented.

Preliminary foaming tests were performed as a part of the initial development of an accurately contoured reflector surface. Results to date and planned future approach are discussed.

The general design approaches for 5-foot-diameter demonstration scale models for the two ground-based AIRMAT antennas are presented. A single curvature inflatable section has been fabricated and has demonstrated the feasibility of utilizing fabric web ribs for the model construction.

PART 3 - PUBLICATIONS, LECTURES, REPORTS, AND CONFERENCES

A conference was held at the U. S. Army Electronics Research and Development Laboratory, Fort Monmouth, New Jersey, on 19 December 1962 with Mr. F. J. Triolo and Mr. F. Kansler of the Astro Electronics Division of USAERDL and W. B. Koller, J. C. Bell Jr., and D. D. Collins, GAC engineering representatives. The purpose of the meeting was to review the results of the second quarter's work on the program consisting of Phase III - Preliminary Analysis and Concept Selection.

The design configurations of the various space vehicle and ground-based antenna concepts were reviewed in detail. The procedure and results of the concept evaluation and selection were reviewed. Tentative selection of the rigid-panel Swirlabola space antenna and two inflatable AIRMAT ground-based antennas for further detail study and model consideration was agreed upon. It was also agreed that ground-based antenna pedestal structures and drives would not be studied extensively, since most of the antenna concepts being considered could be adapted to utilize existing equipment such as the Syncom trailer-mounted pedestal and drive.

The financial report, DD-1097 Report, for November 1962 was submitted to the Signal Corps on 26 December 1962. Reference GAC letter X51-AH1636 of 26 December 1962.

The fifth monthly letter report was submitted to the Signal Corps on 5 January 1963. Reference GAC letter X52-Y2236 of 5 January 1963.

The second quarter financial report, DD-1097, was submitted to the Signal Corps on 24 January 1963. Reference GAC letter X51-Q209 of 24 January 1963.

Draft copies of the second quarterly progress report were submitted to the Signal Corps for review and approval on 30 January 1963. Reference GAC letter X51-G7537 of 30 January 1963.

The sixth monthly letter report was submitted to the Signal Corps on 7 February 1963. Reference GAC letter X51-Q278 of 7 February 1963.

The financial report, DD-1097 Report, for January 1963 was submitted to the Signal Corps on 20 February 1963. Reference GAC letter X51-Q338 of 20 February 1963.

Final approved copies of the second quarterly report were submitted to the Signal Corps on 8 March 1963. Reference GAC letter X51-Y2713 of 8 March 1963.

PART 4 - FACTUAL DATA

SECTION I - PHASE IV - DETAIL STUDY AND ANALYSIS OF SPACE VEHICLE ANTENNA SYSTEMS

A. GENERAL

During the previous quarter, the space vehicle antenna concepts were evaluated and compared on the following basis:

(1) Spectrum of applicability

(2) Weight per unit area, as a function of tolerance steerability and lifetime

(3) Maximum permissible tolerance

(4) Probable cost

The rigid-panel Swirlabola antenna was selected for further detail study and for model design and fabrication.

The following general design goals were established for the Swirlabola antenna:

(1) Simple mechanical structure to enhance reliability.

(2) Lightweight design with close tolerance contour control.

(3) Fabrication methods within the state-of-the-art.

(4) Efficient reflector for r-f energy.

(5) Structurally sound design to withstand handling, repeated erection and storage, launching, and deployment in space.

(6) Type of construction that will maintain mechanical strength and surface accuracies and offer an excellent lifetime with no aging problems.

(7) A solid-skin-type reflector surface with contour accuracies suitable for X-band operation which will be finished to minimize heat concentration on the feed.

(8) A structure fabricated primarily of Invar material to reduce any heating distortion. (Invar has a thermal expansion coefficient of only about 1/10 the value of steel and 1/20 of aluminum.)

(9) Design that permits all necessary alignment adjustments, checkouts, contour measurement, and deployment tests in the factory.

The following general requirements were established as a basis for the design study and analysis:

(1) The erected antenna will provide an essentially circular aperture with an approximate maximum diameter of 10 feet. Its efficiency will be greater than 55 percent.

(2) The antenna will operate at X band. It will use a paraboloidal reflector with an f/D of 0. 3 to 0. 5.

(3) The reflector will have a tolerance of ± 1/12 inch to ± 1/24 inch from a true paraboloidal shape after fabrication and erection, whether in a 1-g or 0-g field at temperatures from -100 to +200°F.

(4) The approximate unit weight of the combined aperture and feed system will be less than 1 pound per square foot.

(5) The antenna will be capable of operating in a search mode, scanning

at a high rate in a sector scan mode about one axis, or scanning slowly and uniformly.

(6) When packaged for stowage, the antenna will fit in the minimum volume, can be erected on the ground, and restowed for space erection.

Detail study and analysis has proceeded along three major areas based on these general goals and requirements:

(1) Electrical design
(2) Structural analysis
(3) Mechanical design

The results to date in these three major areas are discussed in the following paragraphs.

B. ELECTRICAL DESIGN

An aperture efficiency of at least 55 percent, the maximum consistent with the Swirlabola design, has been stipulated.

The primary causes for reduction of aperture efficiency are:

(1) With a conventional feed, it is impractical to produce an illumination of the reflector edges equal to that of the center.

(2) Some energy from the feed system spills over the reflector edges and does not appear in the focused wave.

Several analyses of this decrease in gain are available, and depending on mathematical approximations, indicate that the optimum gain is about 70 percent of that for a uniformly illuminated aperture (Reference 1, p 2-40 and p 12-12). However, experimentally obtained optimum gain figures are on the order of

65 percent (Reference 1, p 2-40 and p 12-12), i. e.

$$G = 0.65 \frac{4\pi A}{\lambda^2}. \quad (1)$$

For small f/D ratios (i. e. for reflectors subtending large angles at the focal point), it becomes difficult to obtain a gain figure as great as 65 percent. The reason for this is apparent from the twofold loss in gain discussed above. For small f/D ratios, a large space attenuation factor reduces edge illumination. This can be seen from Figure 2, where the edge attenuation, A (reference 1, p 12-6), can be found from

$$A = 20 \log_{10} (R/f) = 20 \log_{10} \sec^2 (\theta/2). \quad (2)$$

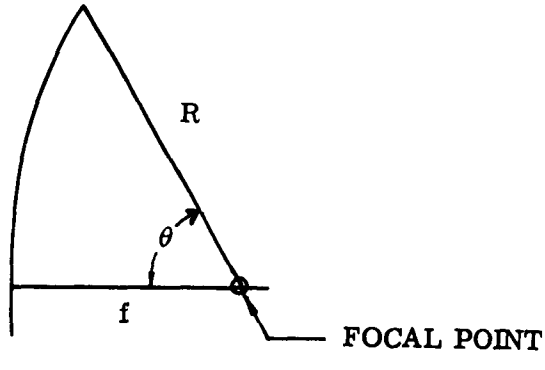

Figure 2 - Edge Attenuation Geometry

Using, for example an f/D of 0.35, it is indicated that θ = 70 degrees, and from Equation 1,

$$A = 20 \log_{10} \sec^2 35 \text{ degrees} = 3.4 \text{ db.}$$

Thus, to obtain an edge illumination of 12 db (usually considered optimum, depending on f/D), the feed pattern in the edge direction can be only 12 db - 3.4 db, or 8.6 db down. The energy below the 8.6-db point is spilled over the edge as a loss.

A good side lobe level can be maintained with the proper edge illumination and minimum mismatch between reflector and feed.

Good design indicates an edge illumination on the order of -20 db for good side lobe performance. To achieve this illumination, a feed horn with a 10-db beamwidth of about 80 degrees is required, with an f/D ratio of 0.5. As the f/D ratio is reduced, the allowable feed beamwidth becomes smaller, since the feed angle corresponding to the reflector edges becomes larger, with a correspondingly larger off-axis space attenuation factor.

For a given reflector, an increase in the gain of the feed will result in greater energy incident upon the reflector vertex, with a correspondingly greater reflected wave and larger mismatch. From these considerations, it can be shown that the reflector coefficient, Γ (Reference 1, p 12-7), introduced by the presence of the paraboloid is given by

$$\Gamma = \frac{g\lambda}{4\pi f} \tag{3}$$

where

g = gain of the feed in the direction of the vertex

and

f = focal length of the reflector.

Considering reflector geometry, it can be shown from Equation 2 that

$$\Gamma \text{ varies in proportion to } \frac{\tan(\theta/2)}{\theta^2}. \tag{4}$$

From Equation 3, it can be seen that smaller value of Γ corresponds to larger values of θ. Moreover, since

$$\text{f/D varies in proportion to } \frac{1}{\tan(\theta/2)}, \tag{5}$$

it is apparent that a good mismatch (low Γ) is obtained with a small f/D ratio. However, there is a limit to reductions in f/D because of corresponding reductions in gain factor. For the present general discussion, therefore, f/D ratios on the order of 0.3 to 0.5 will be considered for the antenna. An f/D of 0.35 has been tentatively established for the Swirlabola antenna.

Some discussion of phase errors or reflector deformations across the antenna surface can be used to establish the basis for specifying antenna tolerances.

For small errors, simplified formulas have been worked out by Ruze (Reference 1, p 2-40) for loss in gain. These are obtained for the limiting cases of small and large correlation intervals (C):

$$\frac{G}{G_0} \approx 1 - \left[\left(\frac{3}{4}\bar{\delta}^2\right)\left(\frac{C^2\pi^2}{\lambda^2}\right)\right] \text{ when } \frac{C}{\lambda} \ll 1 \tag{6}$$

$$\frac{G}{G_0} \approx 1 - \bar{\delta}^2 \quad \text{when } \frac{C}{\lambda} \gg 1 \tag{7}$$

where

$\frac{G}{G_0}$ = gain ratio,

$\bar{\delta}^2$ = rms reflector phase error,

and

C = correlation interval (that dimension, on the average where the errors becomes independent of one another).

The structural configuration of the Swirlabola antenna being considered would indicate large correlation intervals, and as such, Equation 7 would apply. From this type of analysis, it can be shown that antenna distortions at X band must be maintained at ± 1/12 inch to ± 1/24 inch, the latter being the upper design goal for this antenna.

C. STRUCTURAL ANALYSIS

The analysis assumes the following constraints:

(1) X band

(2) Search angle - approximately 22 degrees

(3) Search velocity - 140 degrees/second

These requirements do not completely define the structural problems, but in conjunction with past experience, the requirements provide sufficient information to select the most efficient type of antenna and to approximate its weight and packaging volume.

The Swirlabola is ideally suited for this application. The conventional structure utilized presents a few problem areas. Past experience indicates that the strength required for accelerations, vibration, and shock during boost and in orbit can be met by careful attention to detail design.

The critical problems are associated with the close tolerances required for X band. This requires that deflections of the structure be kept small during the antenna operation. There are two major sources of deflection that must be corrected: those arising from thermal gradients and those arising from the

angular accelerations required in the operating mode. These are subject to trade-offs, and a final design cannot be established until additional requirements are specified. For the present work, a particular design has been selected to provide a basis for discussing the principal trade-off areas and to establish the approximate weight and package volume of the antenna.

The general arrangement of the antenna is shown in Figure 3. The principal structural features include the use of Invar material throughout with 1/2-inch honeycomb panels and 3-inch-diameter ribs.

1. Thermal Deflections

Thermal studies of antennas show that for most missions the surfaces can be treated to control temperatures to acceptable limits. Reasonable limits are a total temperature change of 300°F with temperature differentials across members of 100°F. For this reason, Invar material was selected for its low coefficient of thermal expansion. This coefficient is 0.9×10^{-6} per °F, which is approximately 1/10 and 1/20 the coefficient for steel and aluminum respectively.

The same material is used throughout so that uniform temperature changes will not introduce pointing or focusing errors. Similarity in shape is preserved, and the only effect is a small change in size. For a 300°F temperature change, the change in size will amount to $300 \times 0.9 \times 10^{-6} \times 100 = 0.027$ percent.

Deflections from temperature gradients are a serious problem. Consider a cantilever beam of depth (h) and length (ℓ), initially straight at uniform temperature, then subjected to a temperature differential across the depth of magnitude (T). It can be shown that the deflection at the tip (δ) is

$$\delta = \frac{(\Delta T)\, C\ell^2}{2h} \qquad (8)$$

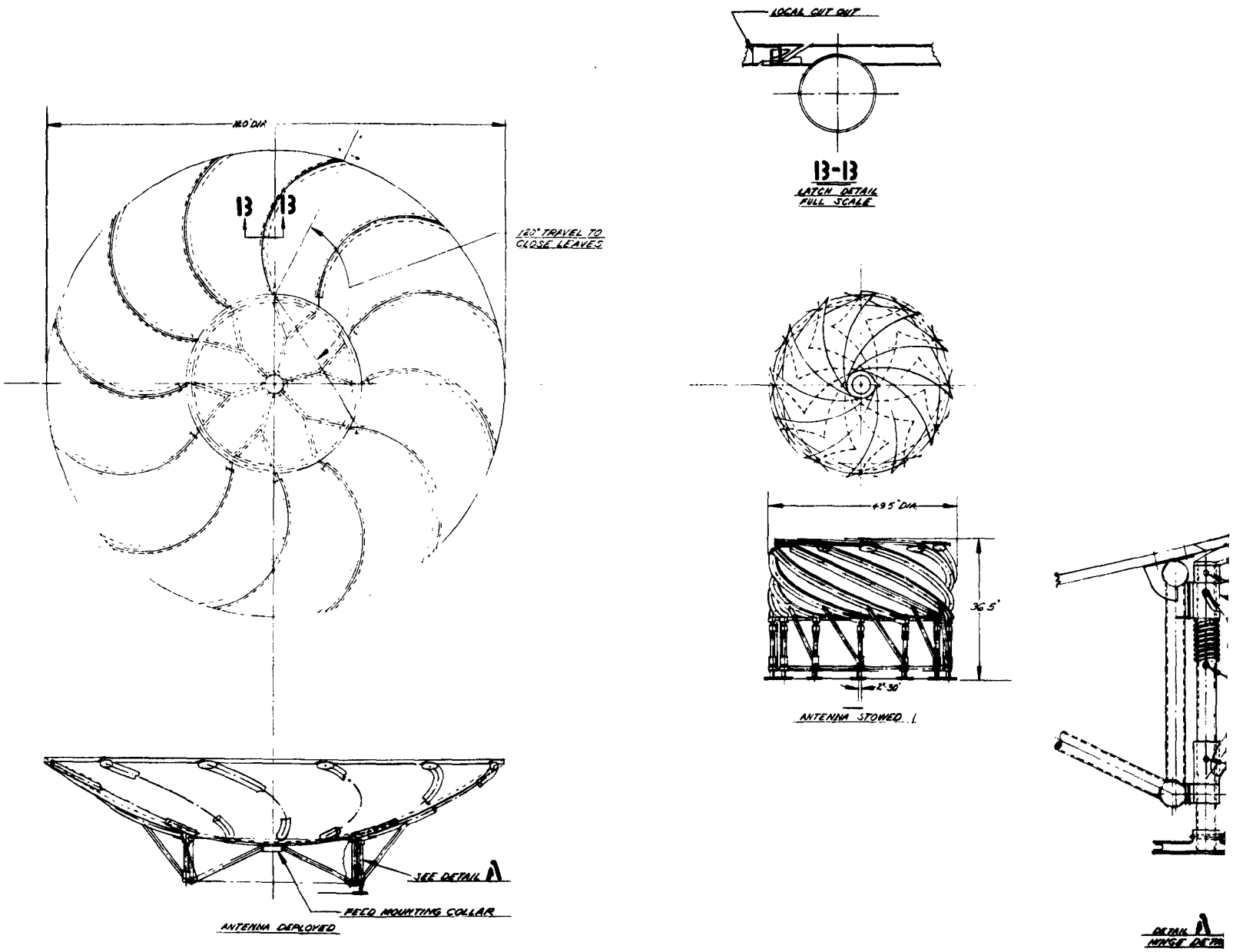

Figure 3 - Rigid-Panel Swirlabola An

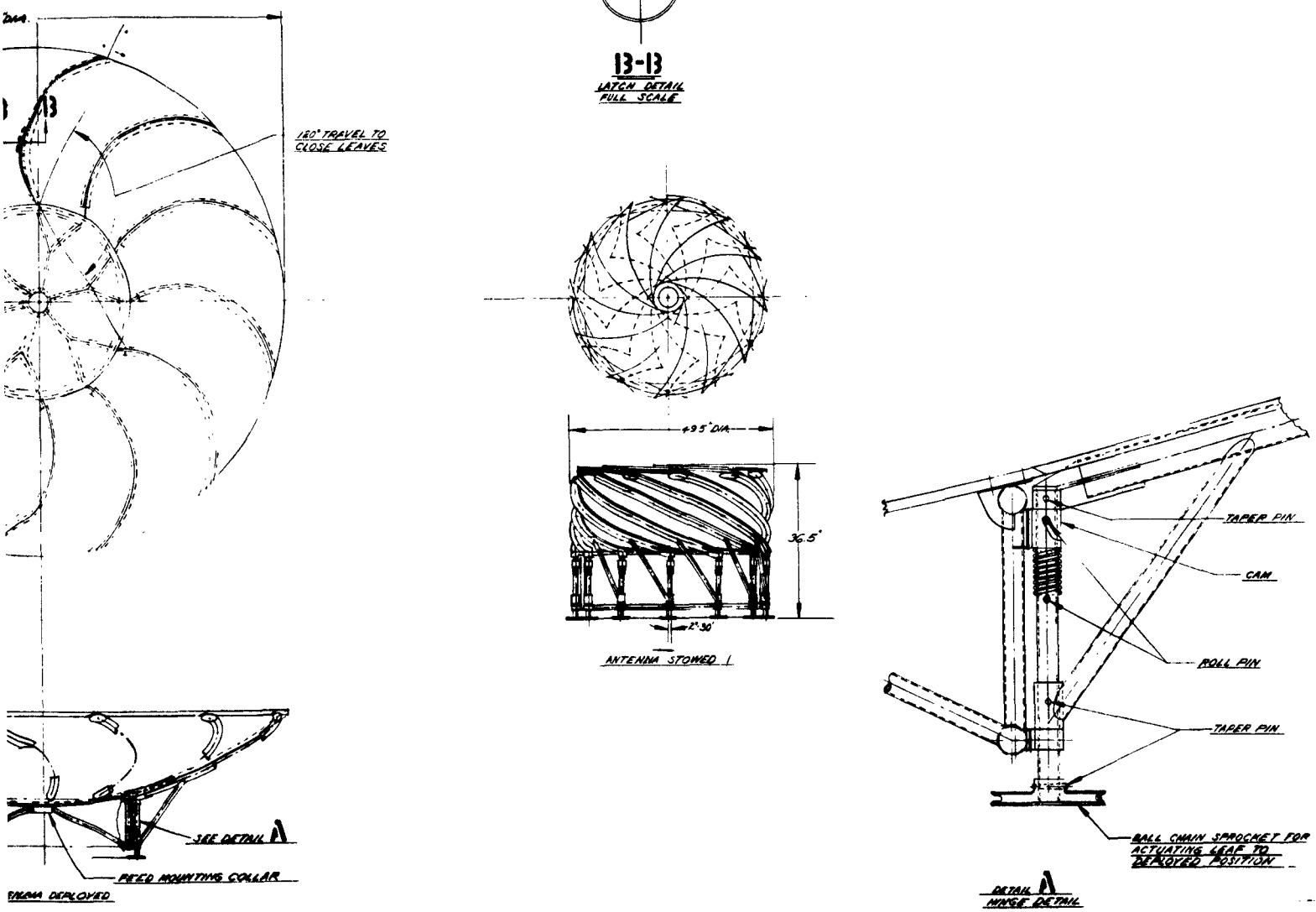

Figure 3 - Rigid-Panel Swirlabola Antenna

where C is the coefficient of thermal expansion. One of the critical deflections is the tip of the rib. The rib is 46 inches long and 3 inches in depth; therefore,

$$\delta = \frac{(100)\ (0.9)\ (10^{-6})\ (46)^2}{(2)\ (3)} = 0.032 \text{ inch.}$$

Another critical deflection is the sandwich panel between the ribs. This is 1/2-inch thick and has a span of about 20 inches between ribs. Equation 8 may be used for this case if ℓ is considered equal to half of the span.

Then

$$\delta = \frac{(100)\ (0.9)\ (10^{-6})\ (10)^2}{(2)\ (1/2)} = 0.009 \text{ inch.}$$

These two deflections are acceptable for X band, whereas if the material were steel or aluminum, the resulting deflections would not be tolerable.

2. Search and Scan Deflections

The turnaround time in the search and scan operations will have a pronounced effect on the weight of the antenna. This is a primary trade-off area and will require considerable study. A study is presented herein.

It is assumed that a sine pulse torque is applied at each end of the stroke to achieve the turnaround. This will result in typical torque and displacement curves as shown in Figure 4. In order to examine the effect of turnaround time on the structure, it is necessary to determine the various quantities shown in Figure 4 in terms of a load factor (n) computed at the tip of the reflector for both the search and scan modes. The angle and velocity in the scan mode are taken as 1/10 of those in the search mode. The resulting expressions are tabulated in Table I, where $r \approx 5$ feet, the distance from the axis of rotation to the tip of the reflector.

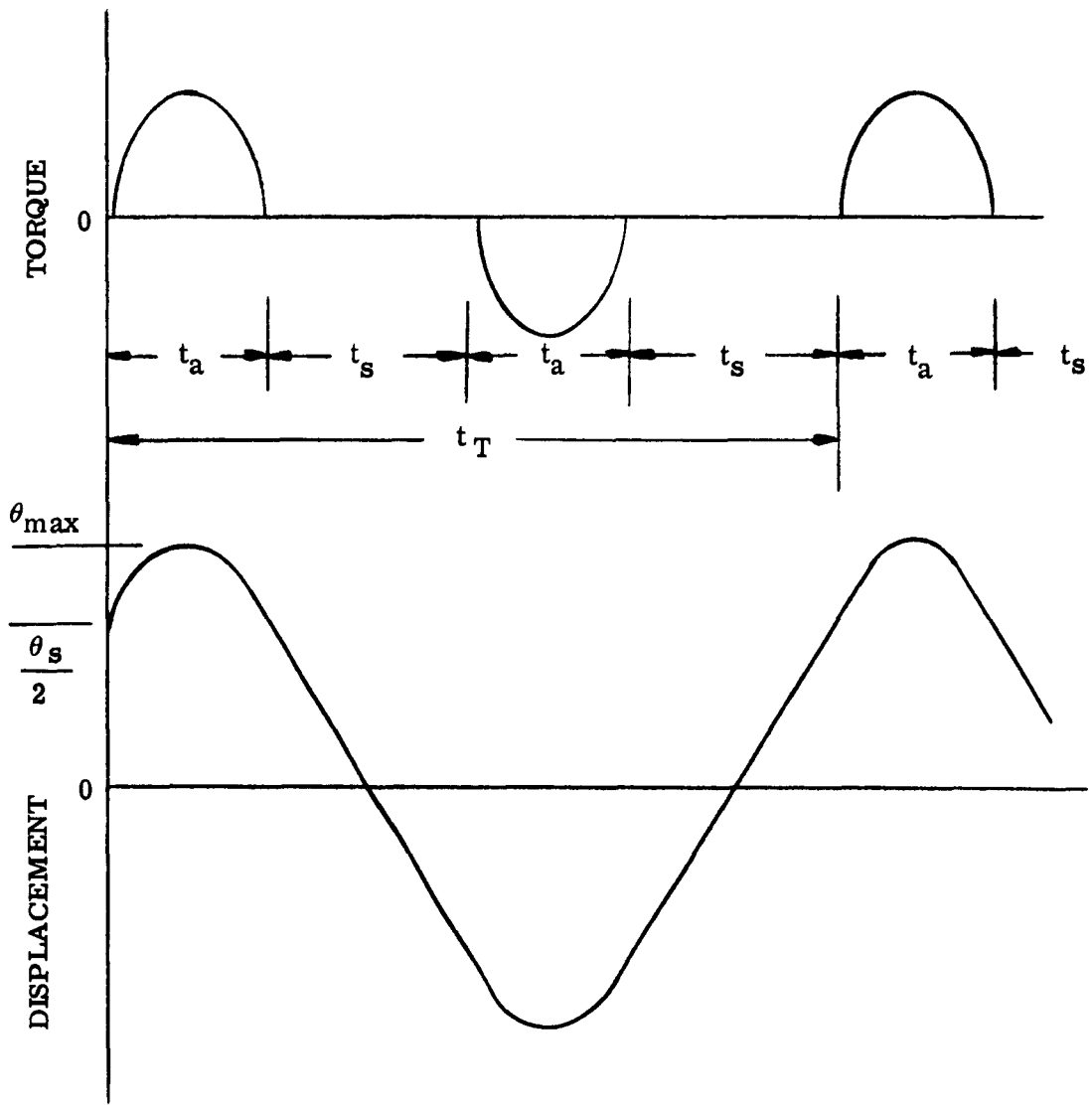

Figure 4 - Typical Torque and Displacement Curves

Table I - Torque and Displacement Parameters for Search and Scan Modes

ITEM	UNITS	SEARCH	SCAN
Scan Angle (θ_s)	degrees	22	2.2
Angular Velocity (W)	degrees/second	140	14
Angular Velocity (W)	radians/second	2.44	0.244
Sweep Time (t_s) = $\frac{\theta_s}{W}$	seconds	0.157	0.157
Turnaround Time (t_a) = $\frac{\pi Wr}{ng}$	seconds	1.19/n	0.119/n
Total Time (t) = $2(t_a + t_s)$	seconds	0.314 + 1.119/n	0.314 + 0.119/n
Overshoot (θ_0) = $\frac{57.3\ W^2 r}{ng}$	degrees	53/n	0.53/n
Maximum Travel (θ_{max}) = $\frac{\theta_s}{2} + \theta_0$	degrees	11 + 53/n	1.1 + 0.53/n

The results for the search and scan modes are plotted in Figures 5 and 6 respectively.

The structural parameters required to complete the analysis were determined for the particular structure selected. These calculations are quite conventional and are not included herein. The principal results are natural frequency with unsymmetrical mode, 32 cps; deflection of rib tip for n = 1, 0.0097 inch; and deflection of sandwich panel between ribs for n = 1, 0.0025 inch.

The major concern is the magnitude of the deflection while the antenna is sweeping across the search or scan angle. The deflection during this time is the residual deflection resulting from the half cycle sine pulse. This deflection depends on the static deflection, which is proportional to the load factor n, and to a response factor dependent on the ratio of the duration of the pulse to the natural period of vibration of the antenna. The response factor for this case is shown in Reference 2. The pulse time is t_a, which was shown in Figures 5 and 6 to be a function of n. The natural period of vibration is the reciprocal of the natural frequency and, for this case, equal to 1/32 or 0.031 second. The residual deflection for the search and scan modes is shown as a function of n in Figures 7 and 8 respectively.

D. MECHANICAL DESIGN

The mechanical design features for the rigid-panel Swirlabola are described in the following paragraphs. At this stage of the program, the configuration is essentially the same as described previously in the second quarterly report.

The antenna configuration (Figure 3) provides 12 curved radial ribs and antenna surface leaves extending from a center hub to the outer periphery, which establish the parabolic contour outboard of the hub. These ribs are pivoted at the hub rim and, having the approximate radius of the hub, nest circumferentially around the hub rim in the packaged condition. The rib structure is

VALUES:

n	t_a	t_T	θ_{max}
2	.595	1.50	37
5	.238	.79	22
10	.119	.55	16
15	.079	.47	14.5
20	.060	.43	13.6

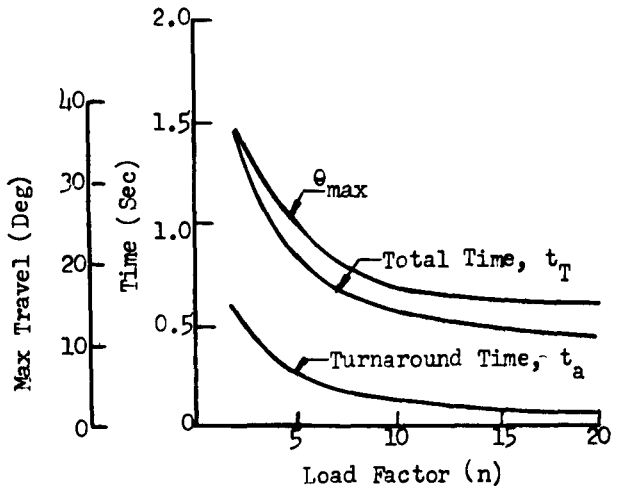

Figure 5 - Turnaround Parameters versus Load Factor (Search Mode)

VALUES:

n	t_a	t_T	θ_{max}
1/2	.238	.280	2.16
1	.119	.552	1.63
2	.060	.433	1.37
5	.024	.362	1.21
10	.012	.339	1.15

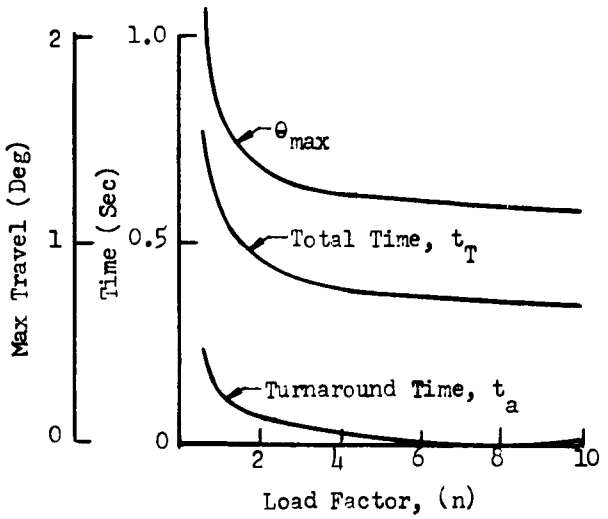

Figure 6 - Turnaround Parameters versus Load Factor (Scan Mode)

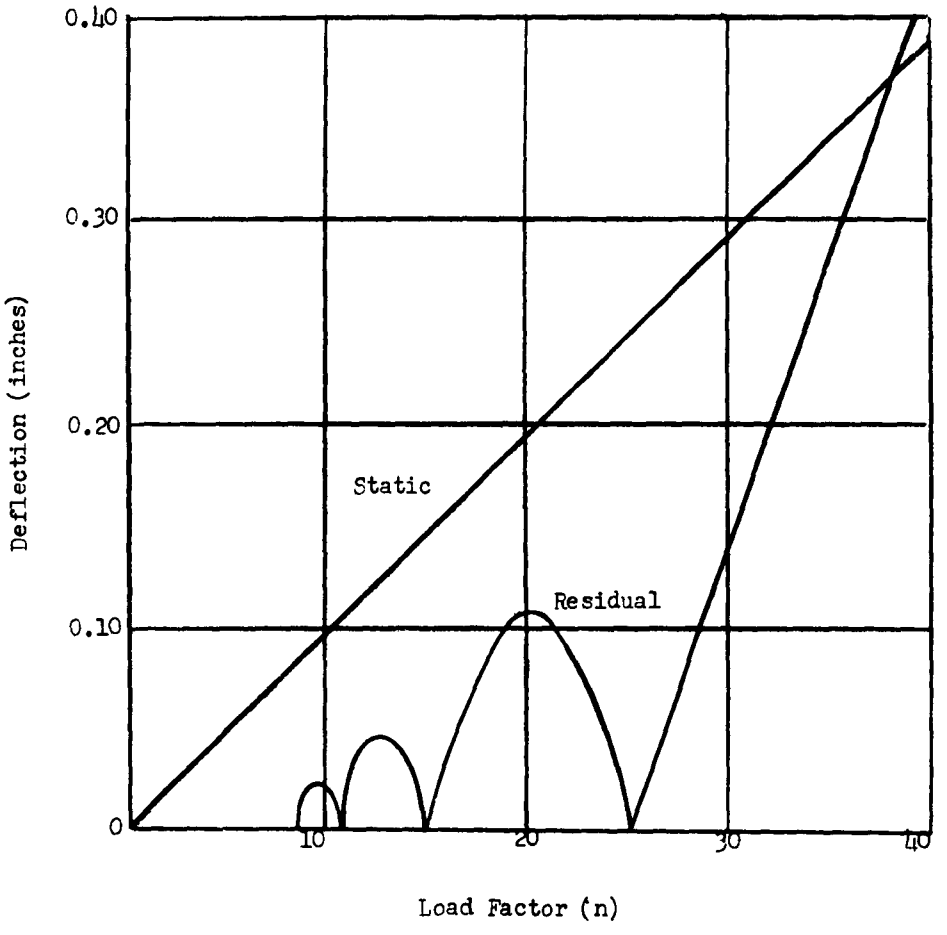

Figure 7 - Residual Deflection for Search Mode

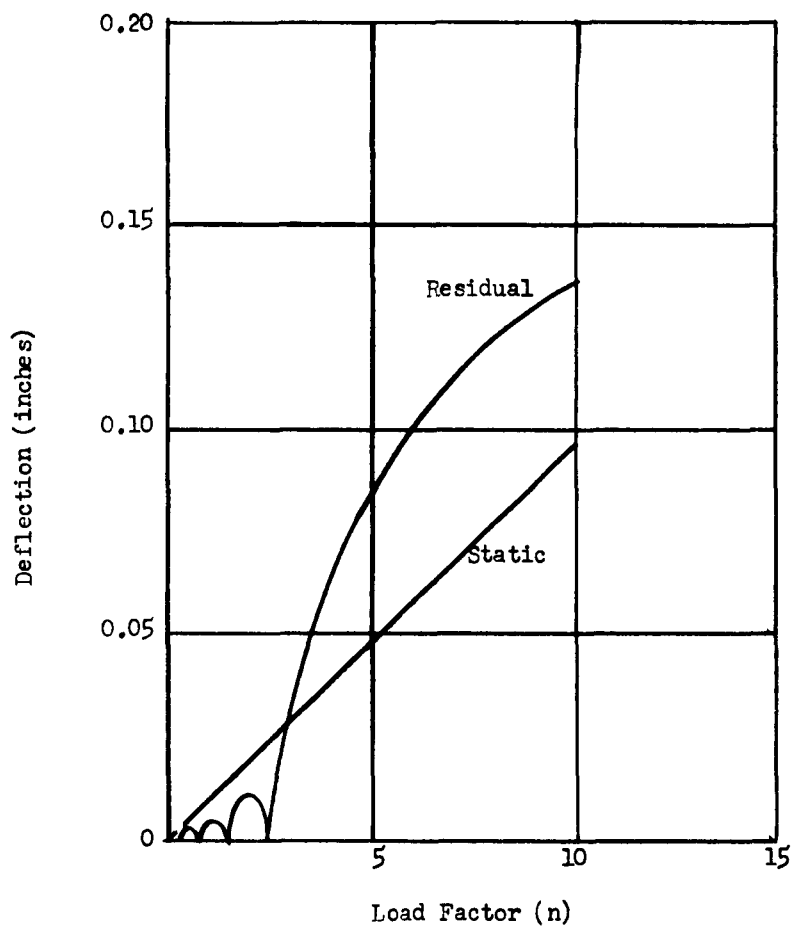

Figure 8 - Residual Deflection for Scan Mode

fabricated of Invar tubes that are chem-milled to reduce the wall thickness as they approach the outer periphery of the reflector.

The outer leaves of the parabolic surface are fabricated of honeycomb sandwich. The sandwich has Invar foil face sheets with Invar honeycomb core. The face sheets, core, and support rib are bound into one integral component. The leaves and ribs are hinged at the central hub (see detail A of Figure 3).

The top pillow block of the hinge also acts as a cam to control the displacement of the leaf during deployment. A compression spring holds the cam pin in the secured position after deployment. Two latches are provided to secure each leaf to its adjacent leaf (see Section B-B of Figure 3). These latches are located at the midpoint of the leaf and at the outboard extremity. The leaves are deployed by a ball chain that drives sprockets at each leaf hinge. The ball chain is spring-loaded to provide constant tension. The prime mover that drives the chain can be either a small electric drive or a pneumatic motor powered by compressed gas. Limit devices can be provided to define the end of travel of the mechanism.

The hub structure will have a supporting space frame of welded Invar tubes. Two tubes are rolled to a 44-inch diameter. Spacer tubes are then welded at each hinge point and have provisions for mounting the pillow blocks for precise position. The hinge center line is canted at $2^{\circ}3'$ so that the folded leaves of the reflector surface will nest on top of each other (see view of the stowed antenna, Figure 3).

The reflector surface for the hub is a honeycomb sandwich composed of Invar face sheets and Invar foil honeycomb core. The sandwich, attached to the hub ring with Invar clips at each hinge location, will serve as the shear resistant member for the hub structure as well as the reflector surface. A spider of Invar tubes spans the distance from the outer ring lower tube to an Invar collar

at the center of the reflector, which also serves as the mounting reinforcement for the feed.

Design features of this antenna will be developed in further detail during the design, fabrication, and evaluation of the scale model. The full-scale design concept will be reviewed during the model program, and the design will be modified as deemed necessary as a result of the experience gained with the model.

A conventional sealed monocoque construction of magnesium can be custom-designed to provide the antenna packaging envelope. It is so designed that the canister cover will slip over the antenna and mount to the interface structure. The canister interface to payload either can be mounted to concentrated load points or can be uniformly distributed, whichever is most favorable to the payload structure.

The canister cover can be jettisonable externally in three sections. A circular clamp of wedge-type cross section is used to secure the cover in the packaged state. Explosive bolts tie the clamp sections together at each of the three cover section separation points. As it is mandatory that the covers be jettisoned and not foul with the canister contents, the three sections are spring-loaded for positive reliable separation. The deployment of the canister cover is initiated by a programmed signal.

Other prime considerations that will influence the canister design are as follows:

(1) The launch environment imposes the effects of shock, vibration, and inertial loads.

(2) The thermal effects at launch and aerodynamic heat effects must be investigated to determine the optimum insulation required for protection of the canister contents.

The canister detail design would be dependent on the configuration of the particular vehicle in which the antenna would be used and on the environmental conditions imposed by that vehicle. Therefore, the design of the canister will not be pursued in further detail in this program.

PART 4 - FACTUAL DATA

SECTION II - PHASE V - MODEL DESIGN AND FABRICATION OF SPACE VEHICLE ANTENNA

A. GENERAL

It was originally planned that Phase V, Model Design and Fabrication, would start at the beginning of the fourth quarter. However, it was deemed desirable to start the model design concurrent with the latter part of Phase IV, Detail Study and Analysis, during the third quarter in order to allow additional time to evaluate the model and resolve any unforeseen problems. Accordingly, design for the scale-model rigid-panel Swirlabola has proceeded during this quarter. The configuration is described in the following paragraphs.

B. MODEL CONFIGURATION

The antenna model will consist of 12 contoured petals and will measure 36 inches in diameter when deployed. The parabolic reflector will have an f/D of 0.35. The packaged diameter will be approximately 14 inches.

Essentially, the model configuration will be the same as shown in Figure 3, except for size reduction (3/10 scale) and modifications to the basic hub and the rotating hinge portion of the petals. The model will be handcrank-operated and will be reversible. The handcrank will drive a combination screw and bellcrank mechanism, which in turn drives a circumferential ring that will simultaneously actuate all 12 petals. The materials being used in the model construction will not represent or simulate scaled-down material gauges and weight proportional to the antenna size. Materials were selected to withstand handling and demonstration of the completed model. It is intended that

the scale model will demonstrate concept feasibility, including packaging and deployment capability and contour accuracy.

PART 4 - FACTUAL DATA

SECTION III - PHASE IV - DETAIL STUDY AND ANALYSIS OF GROUND-BASED TRACKING ANTENNAS

A. GENERAL

The general approach during the past quarter has been to further investigate the AIRMAT paraboloid antenna and the lenticular AIRMAT antenna. The purpose of this investigation was to technically develop the concepts to determine what problem areas exist, if any, and to establish the advantages of each concept.

In addition to design studies on the antenna concepts, Phase V was initiated in February 1963, even though it was not scheduled to begin until 1 March 1963. It was found that perhaps more time would be needed to fabricate the models than initially planned and that the model work would also contribute to the full-scale antenna study and analysis. This item will be discussed further in Section IV.

B. AIRMAT PARABOLOID ANTENNA DESIGN

Three basic areas of investigation are being considered in the design of the AIRMAT paraboloid antenna. These areas are the electrical design, the structural analysis, and the mechanical design.

To date, the electrical design has attempted to establish a design for a maximum gain antenna configuration as well as an optimum design based on mechanical and electrical considerations. Further consideration will be given to the phase delay angles and the phase variation across the dish aperture.

However, no serious electrical problems are anticipated in this concept.

The structural analysis conducted has indicated that the application of diagonal drop threads to an AIRMAT structure offers additional substantiation that an AIRMAT paraboloid antenna can be built to operate as a Class III antenna system.

The mechanical design has not turned up any significant problem areas, and indications are that there are possibly several methods of fabrication that can be utilized. These methods are very practical from an economic standpoint and a technical viewpoint. So far, the problems involved appear to be minor.

Although a considerable amount of development yet remains, the AIRMAT paraboloid antenna concept still appears to offer very good potential as a large, highly mobile tracking antenna.

1. Electrical Design Considerations

The electrical design for the AIRMAT paraboloid was based on a 40-foot-diameter Class III Cassegrain antenna.

An attempt was made to establish a maximum gain antenna configuration as well as an optimum design based on mechanical and electrical considerations. With an f/D (ratio of focal distance to aperture size) of 0. 35, a hyperbolic secondary reflector 1. 6 feet in diameter was selected for the maximum gain configuration. This dish size was established in conjunction with the minimum blockage design requirement and a realistic feed horn design.

For the maximum gain antenna configuration, it appears difficult to keep the location of the single-frequency feed horn within the antenna hub and behind the surface of the paraboloid. The feed horn in this case would be eight feet

long, which is excessively long. Therefore, a seven-foot focal length was used, yielding a more practical feed horn length of 3. 55 feet.

Assuming a 10-db illumination taper, and a 55 percent efficiency, the AIRMAT paraboloid antenna will have a gain of 59. 5 db, not considering blockage effects. The addition of blockage effects would then result in a new gain of 59. 47 db. The effect of the 1. 6-diameter secondary reflector blockage on the side lobe level is shown in Figure 9. Also, for comparison, the blockage effects of a 3. 3-foot-diameter subdish is shown which would represent an optimized antenna configuration. Although no specific side lobe level has been selected for this antenna, it can be seen from Figure 9 that with a dish of this size, the blockage does not begin to affect the side lobe level seriously until the design level is between 40 to 50 db. Obviously, in practice, this side lobe level is rarely considered. At this point it can be seen that some increase in the secondary dish size would not be too degrading to the side lobe level.

The secondary dish support structure has not been included as part of the above blockage consideration; however, several types of support methods are presently under consideration. Some of the types being considered include a rigid multistrut support, an inflatable cylinder support utilizing stabilizing cables, and an inflatable cone support also with stabilizing cables. The rigid fiberglass cylinder support, as shown in Figure 31 of the second quarterly report, was eliminated because of the r-f transmission problems it would create.

In addition to the blockage and the r-f transmission problems, the secondary dish support is also being considered in terms of the phase delay angles and the phase variation across the aperture. However, a detailed study of phase shift variation would be beyond the scope of this program.

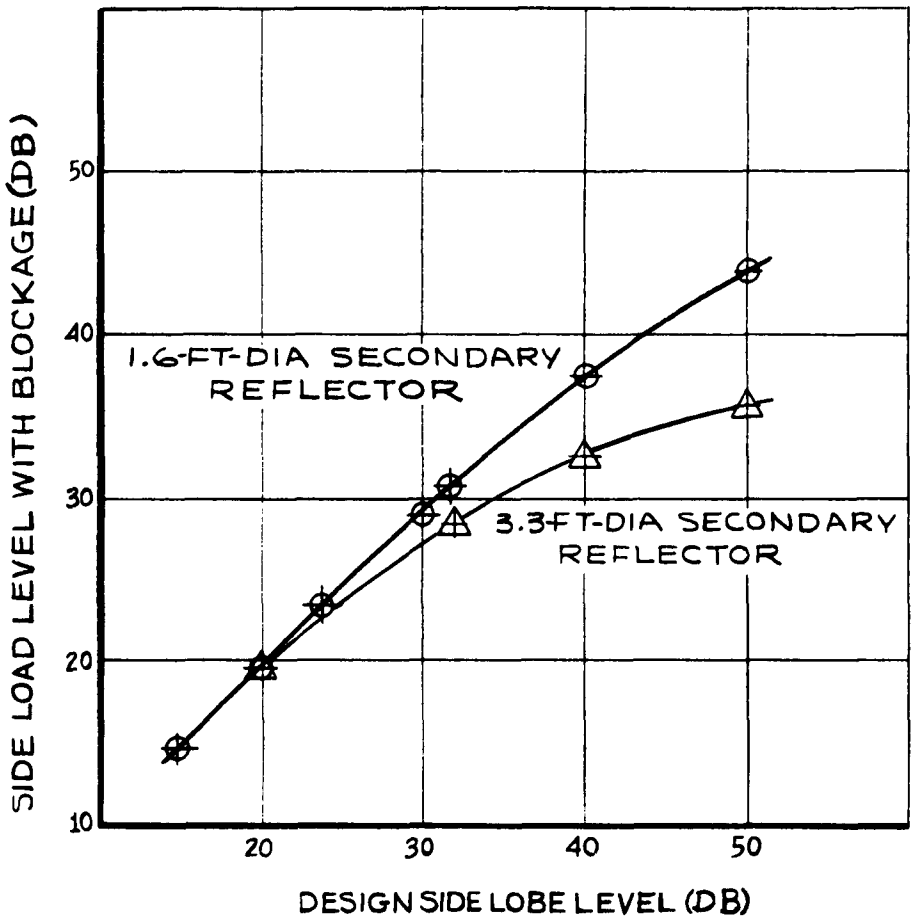

Where

$$\text{Side lobe level with blockage} = 20 \log \left[\frac{\frac{E_s}{E_m} + 2B^2}{1 - 2B^2} \right]$$

$$\frac{E_s}{E_m} = \frac{\text{Side lobe level voltage}}{\text{Main beam voltage}}$$

$$B^2 = (\text{Linear blockage ratio}) = \frac{\text{Blockage area}}{\text{Main dish area}}$$

Figure 9 - Effects of Blockage on Side Lobe Level

2. AIRMAT Paraboloid Deflection Analysis

The AIRMAT paraboloid deflection analysis was made to assist in establishing the structural configuration and the type of material required to limit the antenna deflections within the specified limits for a Class III antenna.

Since the AIRMAT paraboloid antenna will be the first application of diagonal drop threads in AIRMAT structure, a very extensive stress and deflection analysis could be made on this antenna configuration. To minimize expenditures and to reduce the amount of effort required for this analysis, several simplifying assumptions have been made. However, the assumptions made are mostly conservative in nature; therefore, they do not affect the results adversely, since we are attempting to determine the feasibility of the concept. The first assumption is that this deflection analysis is based on a circular flat plate instead of a paraboloid. This flat plate assumption is conservative since a paraboloid dish is inherently a better structure than a circular flat plate. The second assumption is that a constant AIRMAT thickness is assumed. This assumption is not critical since the AIRMAT thickness can be any thickness that is desired. However, in the actual design, the thickness would probably be tapered, since the same thickness at the edge of the dish would not be required to resist bending and shear deflection as is required near the antenna hub. Another assumption is that 96 pairs of radial warp wires and their drop wires are considered as cantilevered from the center hub. In this case, actually more than 96 radial wires would be utilized; some additional support would be provided by the adjacent radial members, and some hoop tension would be carried in the AIRMAT skins.

Two antenna sizes were analyzed here: a 40-foot-diameter antenna and a 20-foot-diameter antenna. These antennas are discussed in the following paragraphs.

a. Forty-Foot-Diameter Reflector. The primary structure is a metal AIRMAT composed of stainless steel warp and fill wires of equal diameter, d_c, and slanted stainless steel drop threads of diameter d_d. The warp wires of the cover plies are oriented along radial lines, and the fill wires form a series of circular hoops to provide hoop tension and compression carrying ability. Ninety-six pairs of radial warp wires and their rows of drop wires are considered as cantilevered from an 8-foot-diameter hub as shown in Figures 10 and 11. The AIRMAT depth is taken as 5 feet, so that there are essentially 96 radial trusses 16 feet long and 5 feet deep.

The 4-inch spacing of the hoop wires is compatible with the spacing of the drop wires and has been chosen as a realistic minimum spacing from a fabrication viewpoint. The resulting hoop stiffness should be more than adequate for deflections due to symmetrical loadings. This analysis for the antisymmetrical part of the loading is then conservative, since the spacing of the hoop wires may probably be increased and/or their diameters decreased. On the other hand, the excess weight of the hoop wires may very possibly be compensated for by the weight of bias plies required for shear stiffness under shear and torsional loadings, which are not considered in this preliminary analysis.

The slanted drop threads (or diagonals of the radial trusses) provide shear stiffness and hold the cover plies the prescribed distance apart. The angle, θ, between the drop thread and the normal to the surface is taken as 33.7 degrees, which results from an interval of every 10 of the 4-inch spaces as shown in Figure 11. This arrangement requires the attachment of 10 pairs of drop wires along the length of the hub and adequate tie off at the tip of the beam to obtain complete efficiency of the slanted drop wires.

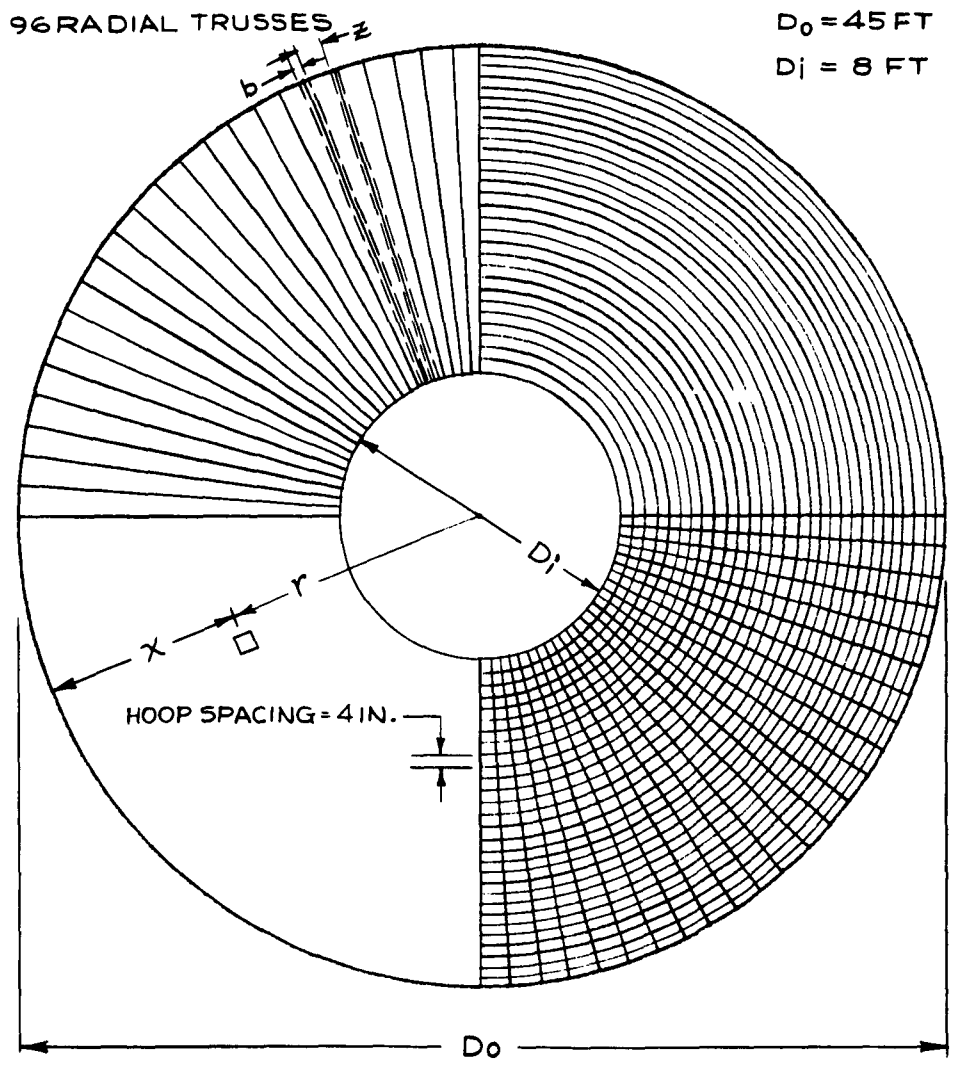

b = RADIAL RIB SPACING AT HUB = π INCHES
z = RADIAL RIB SPACING AT OUTER EDGE (40FT DIA) LESS SPACING AT HUB = 4π INCHES

Figure 10 - Primary Structure Configuration

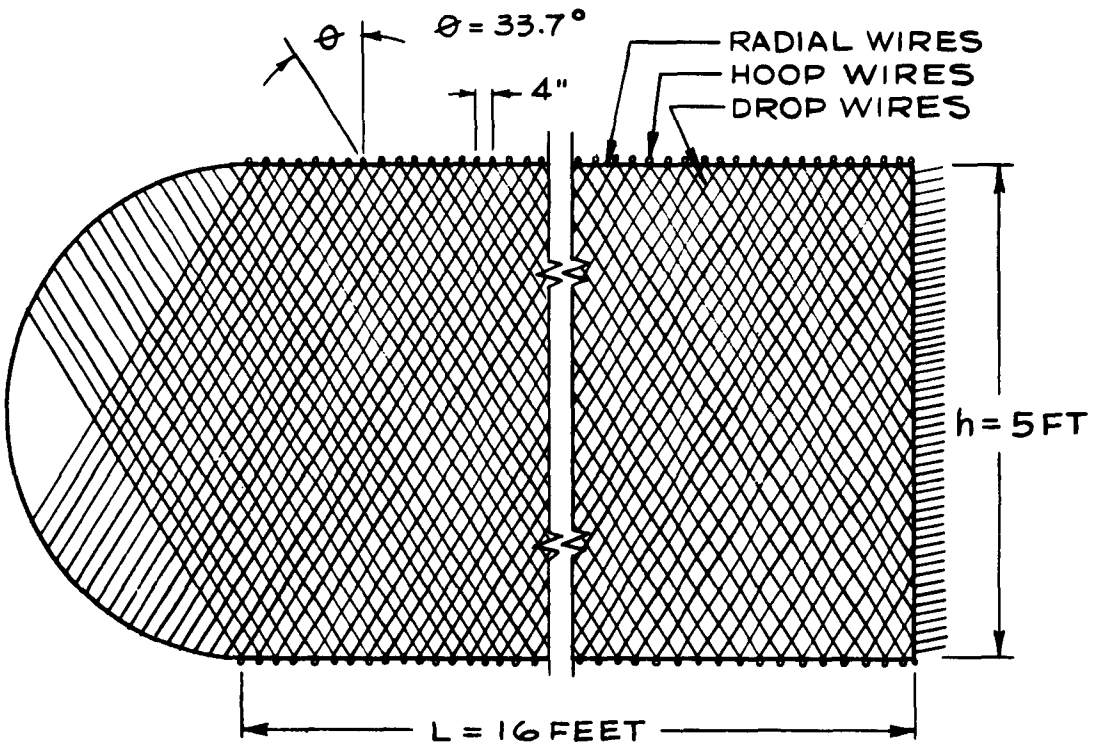

Figure 11 - One Radial Truss

(1) Loads. Consider the loaded area supported by one radial beam. This trapezoidal area is divided into a rectangle of area, A_r, of width, $b = \pi$, and length, L; and a triangle of area, A_Δ, of altitude, $Z = H\pi$, and base, L. Then, from Figure 10, the running load per foot on the beam is

$$w_r = (\pi/12)\gamma = 0.262\,\gamma \text{ lb/ft} \tag{9}$$

$$w_\Delta = \frac{2\pi r - 8\pi}{(96)}\gamma = \frac{\pi(r-4)}{48}\gamma \text{ lb/ft},$$

or in terms of x,

$$w_\Delta = \frac{\pi(16-x)}{48}\gamma = 0.0656(16-x)\gamma \text{ lb/ft} \tag{10}$$

where γ = unit weight in lb/ft^2.

Unit Weight Estimate

For 1/2 in. of 5-pcf foam,	$\gamma_f = 0.2$ lb/ft^2
Assume that weight of reflective surface is	$\gamma_c = 0.07$ lb/ft^2
Steel hoop wires at 4-in. spacing (2 sides), where A_c = cross-sectional area of one wire in in.^{2},	$\gamma_h = 20.4\,A_c$ lb/ft^2
Fabric required to contain inflation gas is assumed equal to hoop wire weight, or	$\gamma_n = 20.4\,A_c$ lb/ft^2
Estimating 15 percent of $(\gamma_h + \gamma_n)$ for seams,	$\gamma_s = 6.2\,A_c$ lb/ft^2
Total,	$\gamma = 47\,A_c + 0.27$ lb/ft^2 (11)

Unit Beam Weight Estimation

2 radial wires, $w_r = 24(0.283)\,A_c$ $= 7\,A_c$ lb/ft

Drop wires, $w_d = (20)\,(2/\sin 33.7^{\circ})(0.283)\,A_d$ $= 123\,A_d$ lb/ft

Drop wire connections (estimated as 5 percent drop wire weight), $w_c = 0.05\,(123\,A_d)$ $= 6\,A_d$ lb/ft

Total unit truss weight, w_t, $= 129\,A_d + 7\,A_c$ lb/ft (12)

Inertia Loads

For the specified acceleration of $6^{\circ}/sec^2$ and for the truss ($\alpha = 6\pi/180 = 0.105$ rad/sec^2), the inertia loads are by Equations 9 and 10

$$w_{rg} = (0.262)\,(0.105/32.2)\,(20 - x)\gamma = 0.000855\,(20 - x)\gamma \text{ lb/ft} \quad (13)$$

$$w_{\Delta g} = (0.0656)\,(0.105/32.2)\,(20 - x)\,(16 - x)\,\gamma = 0.000214\,(20 - x)\,(16 - x)\gamma \text{ lb/ft} \quad (14)$$

$$w_{tg} = (0.105/32.2)\,(20 - x)\,w_t = 0.00326(20 - x)\,w_t \text{ lb/ft.} \quad (15)$$

The antisymmetrical loading condition is now considered. The beam is divided into 2-foot increments, and the combined concentrated normal and tangential loads on each increment are determined in Table II by considering the approximate slope at each increment for a paraboloid of focal length, f = 14.3 ft (see Figure 12).

The parabola is defined by

$$r^2 = 4fy = 4(14.3)y = 57.2y. \quad (16)$$

The slope is

$$\phi = \tan^{-1}(r/28.6). \quad (17)$$

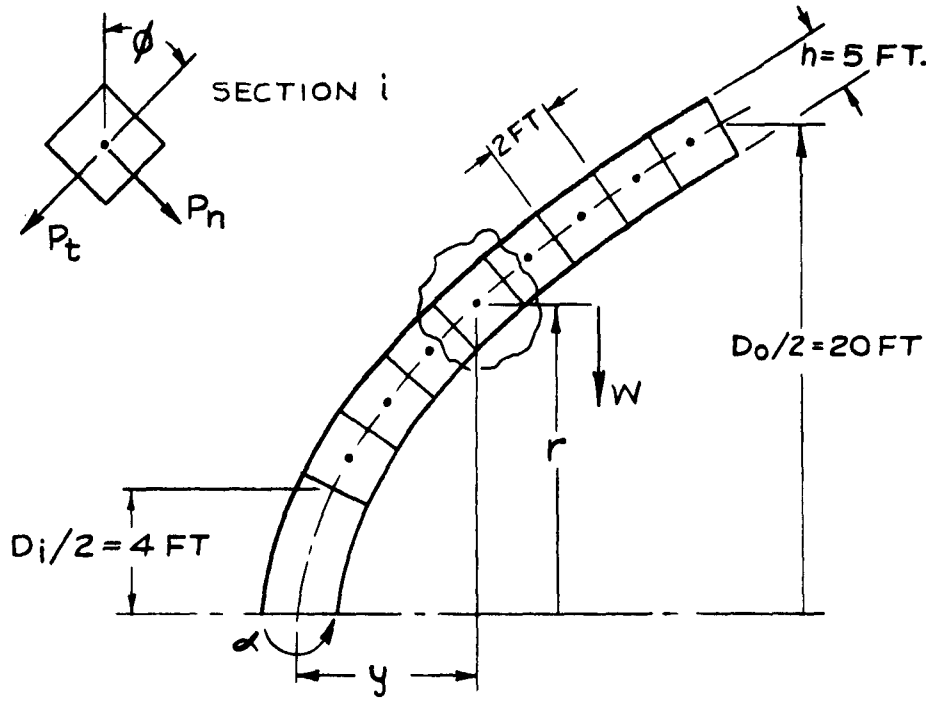

Figure 12 - Antisymmetrical Loading of Critical Radial Beam

(2) Deflections. The wire diameters will first be determined on the basis of bending and shear deflections due to the normal loads for the specified allowable tip deflection of 0.03 inch. The tangential loads (or axial loads) will then be applied to the deflected beam, and new deflections will be determined. The added deflection due to this column effect will be small; otherwise the axial loads would be in the same order of magnitude as the critical buckling load for the column. Hoop stiffness is neglected.

The moments (M_n), area of the moments (A_{M_n}), and moments of the area of the moments ($M_{A_{M_n}}$) due to the normal loads of Table II are determined in Table III.

The bending deflection at the tip of the beam is

$$\Delta_{bt} = \frac{\Sigma M_{A_{M_n}}}{E_c I} = \frac{3456}{E_c A_c h^2} (4316.6 w_t + 4587.6 \gamma) \text{ in.} \quad (18)$$

or

$$\Delta_{bt}(E_c A_c h^2) \times 10^{-6} = 14.9 w_t + 15.9 \gamma \quad (19)$$

where

h = in.

A_w = in.^{2}

E_c = psi

w_t = lb/ft

γ = lb/ft^2

Table II - Combined Normal and Tangential Loads

(1) x	(2) Approx r	(3) ϕ	(4) $P_{w\Delta}$ (by Eq 10)	(5) P_{1g}	(6) P_t = (5) cos (3)	(7) P_{n1g} = (5) sin (3)	(8) P_n = (7) + Eq 13, 14, and 15
0	19	$33^{o}37'$	1.968γ	$2w_t + 2.492\gamma$	$1.665w_t + 2.075\gamma$	$1.11w_t + 1.385\gamma$	$1.234w_t + 1.54\gamma$
2	17	$30^{o}45'$	1.705γ	$2w_t + 2.229\gamma$	$1.72w_t + 1.92\gamma$	$1.025w_t + 1.14\gamma$	$1.136w_t + 1.264\gamma$
4	15	$27^{o}42'$	1.443γ	$2w_t + 1.967\gamma$	$1.775w_t + 1.745\gamma$	$0.93w_t + 0.915\gamma$	$1.028w_t + 1.011\gamma$
6	13	$24^{o}28'$	1.181γ	$2w_t + 1.705\gamma$	$1.823w_t + 1.55\gamma$	$0.828w_t + 0.706\gamma$	$0.913w_t + 0.778\gamma$
8	11	$21^{o}\ 3'$	0.918γ	$2w_t + 1.442\gamma$	$1.87w_t + 1.35\gamma$	$0.719w_t + 0.518\gamma$	$0.791w_t + 0.570\gamma$
10	9	$17^{o}29'$	0.655γ	$2w_t + 1.179\gamma$	$1.91w_t + 1.135\gamma$	$0.6w_t + 0.354\gamma$	$0.659w_t + 0.389\gamma$
12	7	$13^{o}46'$	0.393γ	$2w_t + 0.917\gamma$	$1.94w_t + 0.89\gamma$	$0.477w_t + 0.219\gamma$	$0.523w_t + 0.239\gamma$
14	5	$9^{o}55'$	0.131γ	$2w_t + 0.655\gamma$	$1.97w_t + 0.645\gamma$	$0.345w_t + 0.113\gamma$	$0.377w_t + 0.124\gamma$
16							
					$\Sigma = 14.63w_t + 11.3\gamma$		$\Sigma = 6.661w_t + 5.915\gamma$

Table III - Bending Deflection Calculations

(1) x	(2) M_n	(3) A_{M_n}	(4) $M_{A_{M_n}}$
0	0	$1.234w_t + 1.54\gamma$	$1.645w_t + 2.06\gamma$
2	$1.234w_t + 1.54\gamma$	$6.072w_t + 7.424\gamma$	$18.716w_t + 22.272\gamma$
4	$4.838w_t + 5.884\gamma$	$15.444w_t + 18.387\gamma$	$77.22\ w_t + 91.935\gamma$
6	$10.606w_t + 12.503\gamma$	$28.921w_t + 33.414\gamma$	$202.447w_t + 233.898\gamma$
8	$18.315w_t + 20.911\gamma$	$46.043w_t + 51.578\gamma$	$414.387w_t + 464.202\gamma$
10	$27.728w_t + 30.667\gamma$	$66.319w_t + 72.049\gamma$	$729.509w_t + 792.539\gamma$
12	$38.591w_t + 41.382\gamma$	$89.227w_t + 94.107\gamma$	$1159.951w_t + 1223.39\gamma$
14	$50.636w_t + 52.725\gamma$	$114.217w_t + 117.156\gamma$	$1713.255w_t + 1757.34\gamma$
16	$63.581w_t + 64.431\gamma$		
			$\Sigma = 4316.630w_t + 4587.636\gamma$

The shear deflection of a standard, cantilevered AIRMAT beam (drop threads normal to the skins) with a concentrated load at the free end is

$$\Delta_S = PL/pbh \text{ (in.)} \qquad (20)$$

where

P = concentrated tip load (lb)

p = inflation pressure (psi)

L = length of the beam (in.)

b = width of the beam (in.)

h = depth of the beam (in.)

For an AIRMAT with slanted drop threads as shown in Figure 11, the shear stiffness, say C, is greatly increased above the stiffness pbh

of Equation 20. The shear stiffness for this construction is given in Reference 3 for a beam of unit width (b = 1 in.) as

$$C = ph + 2mnh\, A_d E_d \sin^2\theta \cos\theta \text{ lb/in.} \quad (21)$$

where

A_d = area of a drop thread (in. ^{2})

θ = angle between drop thread and normal to the surface

$2n$ = total number of drop threads per unit length

m = number of drop threads across the unit width.

For the radial beams, an average width of $b = 5\pi/2 = 7.85$ inches is taken for the pressure term of Equation 21, and is an adequate approximation since this term is very small compared to the second term. Also, in the second term, the product mb is unity for the radial beam. Substituting the above, along with $\theta = 33.7^{\circ}$, into Equation 21 yields

$$C = 7.85\, ph + 2(0.256)nh\, A_d E_d \text{ lb}, \quad (22)$$

or neglecting the first term (slightly conservative),

$$C \approx \frac{nh}{2} A_d E_d \text{ lb}. \quad (23)$$

The shear deflection of each 2-foot increment under the load, P_n, at its midspan is

$$d\Delta_s = \frac{2P_n L}{nhA_d E_d} \text{(feet)}$$

$$= \frac{2P_n}{nhA_d E_d} \text{ (feet) for L = 1 foot,} \quad (24)$$

and the tip deflection is then

$$\Delta_{st} = \frac{24}{nhA_dE_d}\left[\Sigma P_n + 2(i-1)\,P_{n_1} + 2(i-2)\,P_{n_2} + \ldots 2P_{n_{i-1}}\right] \quad (25)$$

where

$i = 8$ for 8 increments of 2 feet each.

Substituting for P_n values for Table II into Equation 25,

$$\Delta_{st}(E_dA_d\,nh) = 1526\,w_t + 1546\,\gamma. \quad (26)$$

Substituting for w_t and γ from Equations 11 and 12 along with $n = 1/4$, $h = 60$, and $E_c = E_d = 29 \times 10^6$ for steel into Equations 19 and 26 yields

$$\Delta_{bt} \times 10^3 = 18.41\,A_d/A_c + 0.0411\;\;1/A_c + 1.00 \text{ in.} \quad (27)$$

$$\Delta_{st} \times 10^3 = 0.1916\,A_c/A_d + 0.00096\;\;1/A_d + 0.4525 \text{ in.} \quad (28)$$

The total primary deflection for the particular case of equal cover ply and drop wires ($A_d = A_c = A$) is

$$\Delta \times 10^3 = (\Delta_{bt} + \Delta_{st}) \times 10^3 = 20.054 + 0.04206/A.$$

Solving for A,

$$A = \frac{0.04206}{\Delta \times 10^3 - 20.054}\ (\text{in.}^2) \quad (29)$$

and the diameter is,

$$d = \sqrt{0.0536/\Delta \times 10^3 - 20.054}\ . \quad (30)$$

The required wire diameters for allowable tip deflections of 0.03, 0.05, 0.5, and 1 inch are calculated in Table IV. Also given are the

corresponding minimum bend radii (ρ) to prevent yielding based on F_{ty} = 100 psi and given by

$$\rho = (Ed)/(F_{ty}) \text{(for a circular section)}, \tag{31}$$

or

$$\frac{\rho}{d} = \frac{29 \times 10^6}{0.2 \times 10^6} = 145. \tag{32}$$

Table IV - Required Wire Diameters for Primary Allowable Tip Deflection (Neglecting Beam Column Effects) for $d_c = d_d = d$ and Minimum Bend Radii

① Allowable, Δ (in.)	② $d^2 = \frac{0.0536}{\Delta \times 10^3 - 20.054}$ (in.^{2})	③ d (in.)	④ $\rho = 145d$ (in.)
0.03	0.005389	0.0734	10.64
0.05	0.00179	0.0423	6.13
0.5	0.0001117	0.0106	1.54
1	0.0000547	0.0074	1.07

The above values are plotted in Figure 13, along with the required cover ply wire diameters, d_c, for several other values of the ratio, $k = d_d/d_c$. The obtainable k values are governed by fabrication and packagability limitations and strength requirements.

Beam column effect, for simplicity, considers only the case of Δ = 1 in. and k = 1. Then from Figure 13, $d_c = d_d$ = 0.0074 in. The corresponding unit weights are from Equations 11 and 12.

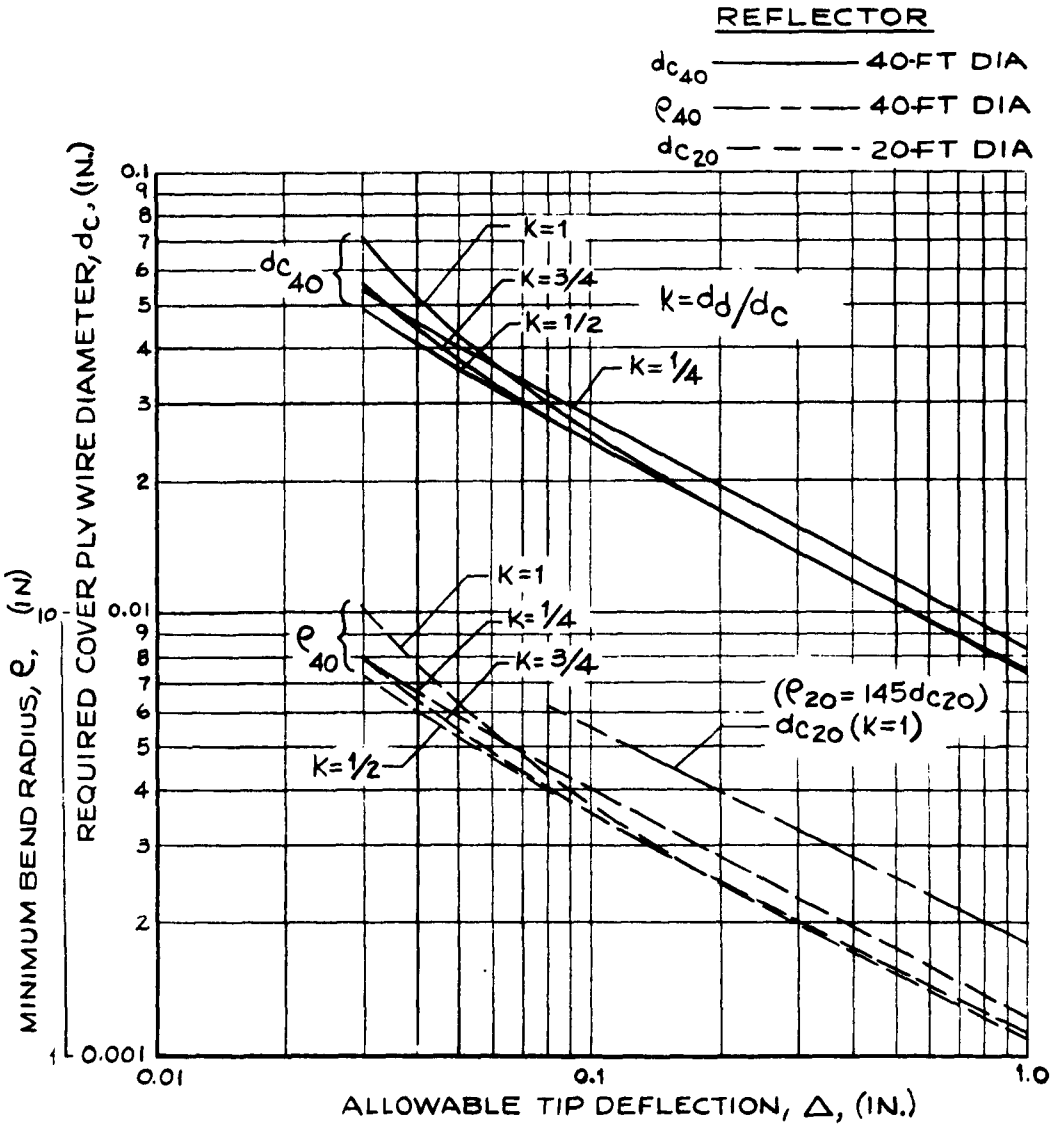

Figure 13 - Required Cover Ply Wire Diameter and Minimum Bend Radius versus Allowable Tip Deflection for Values of the Drop Wire Diameter to Cover Wire Diameter Ratio, k

$$\gamma = (47)(\pi/4)(0.0074)^2 + 0.27 = 0.272 \text{ lb/ft.}^2$$

$$w_t = (129 + 7)(\pi/4)(0.0074)^2 = 0.00585 \text{ lb/ft.}$$

The above values are substituted into the expressions of columns (6) and (8) of Table II, and column (3) of Table III, and recorded in Table V. The deflected curve is determined, the moments due to the axial loads, M_{P_t}, and finally the added tip deflection, Δ_{at}, are calculated in Table V. Again, Equations 18 and 25 are used to obtain bending and shear deflections. Substituting $E = 29 \times 10^6$, $n = 1/4$, $h = 60$, and $A = \pi/4(0.0074)^2 = 43.0 \times 10^{-6}$ into Equations 18 and 25 yields

$$\Delta_b = \frac{3456 \Sigma M_{A_m}}{(29)(43.0)(3600)} = 0.770 \times 10^{-3} \Sigma M_{A_n} \quad (33)$$

$$\Delta_s = \frac{(24)(4) \Sigma P_n}{(60)(43.0)(29)} = 1.283 \times 10^{-3}$$

$$\times \left[\Sigma P_n + 2(i-1) P_{n_2} + \ldots 2 P_{n_{i-1}} \right] \quad (34)$$

where

$i = 8$ for 8 increments of 2 feet each.

The additional tip deflection is (by Equations 33 and 34)

$$\Delta' = \Delta_b' + \Delta_s' = (0.770 \times 10^{-3})(13.62)$$

$$+(1.283 \times 10^{-3})(0.01844 + 0.17674) = 0.0107 \text{ in.} \quad (35)$$

This added deflection is only 1 percent of the primary deflection (1 inch) for the case considered and indicates that these secondary deflections may be neglected for the other cases of Figure 13.

b. Twenty-Foot Diameter Reflector. The effect of the beam length, L, may be quickly estimated on the basis of bending deflections, since the shear deflections are essentially negligible for the slanted drop thread construction in the range of allowable tip deflections of from about 0. 1 to 1 inch, observed in Figure 13 and columns (4) and (7) of Table V.

In order to quickly compare a 20-foot diameter reflector with the 40-foot diameter reflector, the same rectangular loaded area on one beam is used by choosing (for the 20-foot reflector) a hub diameter, D_i = 4 ft, along with 48 radial beams.

Then, from Equations 9 and 10,

$$w_r = 0.262\,\gamma \text{ lb/ft} \tag{36}$$

and

$$w_\Delta = (\pi/24)(8 - x)\gamma = 0.1312(8 - x)\,\gamma \text{ lb/ft.} \tag{37}$$

The unit loads, γ and w_t, are again given by Equations 11 and 12.

The inertia loads to be compared to those of Equations 13 through 15 become

$$w_{rg} = 0.000855(10 - x)\,\gamma \text{ lb/ft} \tag{38}$$

$$w_{\Delta g} = 0.000428(8 - x)\,\gamma \text{ lb/ft} \tag{39}$$

$$w_{tg} = 0.00326(10 - x)w_t \text{ lb/ft.} \tag{40}$$

Assuming the same parabolic shape as in Figure 12 and holding all other parameters for the bending stiffness (EI) constant, the relative tip deflections are determined for the following deflection formulas (see Figure 14):

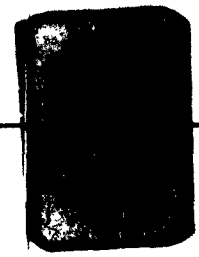

Table V - Secondary Deflection Calculations (Beam Co

(1) x	(2) P_t from (6) of Table II (lb)	(3) P_n from (8) of Table II (lb)	(4) $\Delta_s = 1.283 \times 10^{-3}$ [ΣP_n + Eq 34] (in.)	(5) A_{M_n} from (3) of Table III	(6) $\Sigma M_{A_{M_n}}$	(7) $\Delta_b = 0.770 \times 10^{-3}$ $\Sigma M_{A_{M_n}}$ (in.)	(8) $\Delta = \Delta_s + \Delta_b$ (4) + (7) (in.)	(9) Slope = $\tan \phi' \approx \sin \phi'$	co
0	0.5741	0.4260	0.02291	0.426	1272.955	0.98018	1.003	0.00704	
2	0.5323	0.3505	0.02236	2.055	1053.843	0.81146	0.834	0.00704	
4	0.4850	0.2810	0.02082	5.092	837.212	0.64465	0.665	0.00679	
6	0.4322	0.2170	0.01848	9.258	627.728	0.48335	0.502	0.00638	
8	0.3781	0.1597	0.01549	14.299	432.594	0.33310	0.349	0.00567	
10	0.3172	0.1097	0.01202	19.985	261.017	0.20098	0.213	0.00458	
12	0.2534	0.0681	0.00821	26.119	123.724	0.09527	0.103	0.00308	
14	0.1870	0.0359	0.00417	32.535	32.535	0.02505	0.029	0.00121	
16			0		0	0	0		

Table V - Secondary Deflection Calculations (Beam Column Effect)

(6) $\Sigma M_{A_{M_n}}$	(7) $\Delta_b = 0.770 \times 10^{-3} \Sigma M_{A_{M_n}}$ (in.)	(8) $\Delta = \Delta_s + \Delta_b$ (4) + (7) (in.)	(9) Slope = $\tan \phi' \approx \sin \phi'$	(10) $\cos \phi'$	(11) $P_t' =$ (2)(10) $\approx$ (2) (lb)	(12) $P_n' =$ (2)(9) (9)(11) (lb)	(13) M_n'	(14) $A_{M_n'}$	(15) $M_{A_{M_n'}}$
1272.955	0.98018	1.003	0.00704	1	0.5741	0.00404	0	0.00404	0.0054
1053.843	0.81146	0.834	0.00704	1	0.5323	0.00375	0.00404	0.01991	0.0597
837.212	0.64465	0.665	0.00679	1	0.4850	0.00329	0.01587	0.05061	0.2530
627.728	0.48335	0.502	0.00638	1	0.4322	0.00276	0.03474	0.09440	0.6608
432.594	0.33310	0.349	0.00567	1	0.3781	0.00214	0.05966	0.14914	1.3423
261.017	0.20098	0.213	0.00458	1	0.3172	0.00145	0.08948	0.21237	2.3361
123.724	0.09527	0.103	0.00308	1	0.2534	0.00078	0.12289	0.28142	3.6585
32.535	0.02505	0.029	0.00121	1	0.1870	0.00023	0.15853	0.35371	5.3056
0	0	0					0.19518		
						$\Sigma = 0.01844$			$\Sigma = 13.6214$

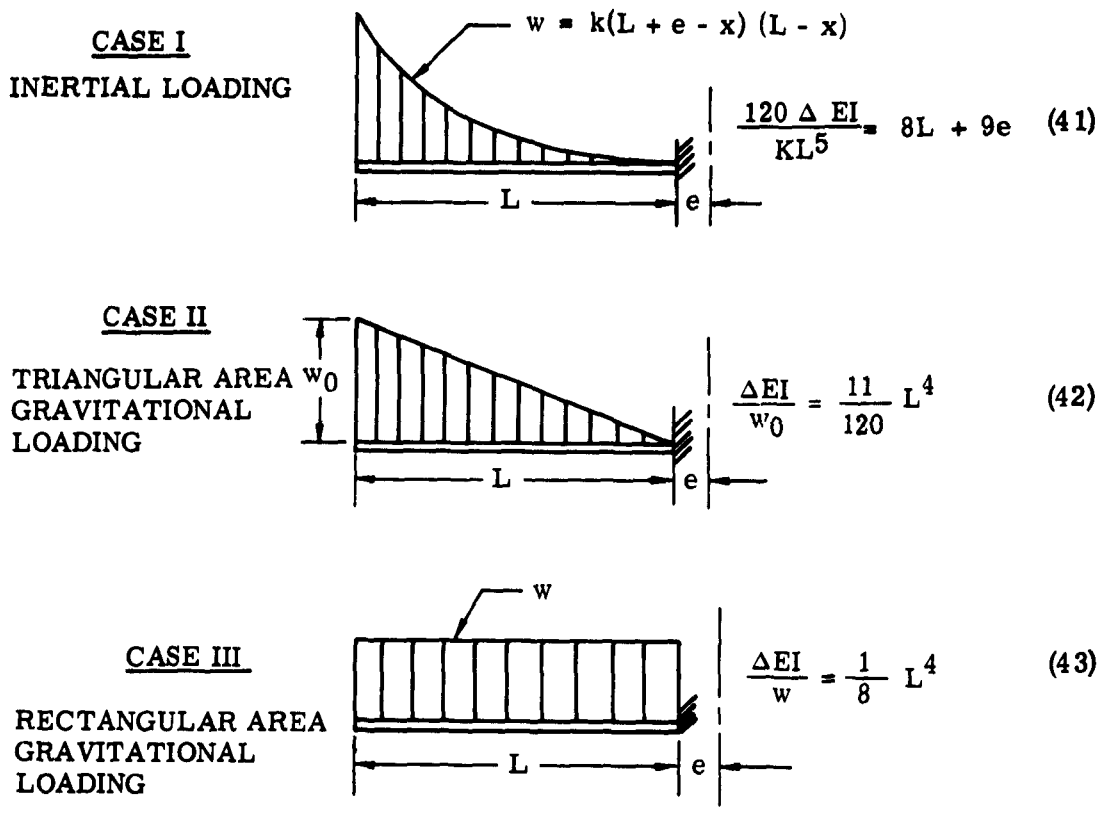

$$\frac{120\,\Delta\,EI}{KL^5} = 8L + 9e \qquad (41)$$

$$\frac{\Delta EI}{w_0} = \frac{11}{120} L^4 \qquad (42)$$

$$\frac{\Delta EI}{w} = \frac{1}{8} L^4 \qquad (43)$$

Figure 14 - Typical Simple Beam Loadings

c. Relative Deflection for the 40-Foot Reflector. Substitution of the loading for the 40-foot reflector into the previous bending deflection equations yields the following:

Equations 9, 12, and 43,

$$EI\Delta_{w_r} = \frac{0.262}{8} \gamma L^4 \qquad (44)$$

$$EI\Delta_{w_t} = \frac{w_t}{8} L^4 \ . \qquad (45)$$

Equations 10 and 42,

$$EI\Delta_{w_\Delta} = \frac{11(0.0656)}{120}\gamma L^5. \tag{46}$$

Equations 13, 15, and 42,

$$EI\Delta_{w_{rg}} = \frac{11(0.000855)}{120}\gamma (L + e)L^4 \tag{47}$$

and

$$EI\Delta_{w_{tg}} = \frac{11(0.00326)}{120} w_t(L + e) L^4 . \tag{48}$$

Equations 14 and 41,

$$EI\Delta_{w_{\Delta g}} = \frac{0.000214}{120}\gamma (8L + 9e) L^5 . \tag{49}$$

Substituting L = 16 ft and e = 4 ft into Equation 44 then 49 along with Equations 11 and 12 for the case of $A_c = A_d = A$ and combining yields

$$EI\Delta = 8861\,\gamma + 8584\, w_t = 1,584,000A + 2,392. \tag{50}$$

d. Relative Deflection for the 20-Foot Reflector. Substitution of Equations 9, 12, and 27 through 40 into the deflection formulas along with L = 8 ft and e = 2 ft, for the case of $A_c = A_d = A$, yields

$$EI\Delta = 541.0\,\gamma + 524.2\, w_t = 96,718A + 146. \tag{51}$$

e. Required Cover Ply Wire Diameter. For the same modulus, beam depth, and allowable deflection, Equations 50 and 51 may be equated after the

substitution of $EI = EAh^2/2$ to obtain

$$1,584,000 + \frac{2,392}{A_{40}} = 96,700 + \frac{146}{A_{20}} \tag{52}$$

where

A_{40} and A_{20} are the required cross-section areas of the cover ply wire for the 40-foot and 20-foot diameter reflectors respectively.

Then

$$A_{20} = \frac{146\ A_{40}}{1,487,300\ A_{40} + 2,392}, \text{ or the required diameter is} \tag{53}$$

$$d_{20} = \sqrt{\frac{146\ d_{40}^2}{1.168,100\ d_{40}^2 + 2,392}}\ . \tag{54}$$

Equation 54 is also plotted in Figure 13 for values of d_{40} taken from Figure 13 in the range $0.1 < \Delta < 1$, where shear deflections are negligible. Also, as an added assist in using the curves in Figure 13, it must be recognized that the wire sizes given by the curves are based on 96 radial wires. If additional radial wires are provided, the diameter of the wires is reduced, since it is actually the total cross-sectional area of the wires that is required rather than the actual size of the wire. For this same reason, the ordinate giving the minimum bend radius also does not apply except when only 96 radial wires are used. In most practical applications more than 96 wires would be used. The 96 number was only used as one of the initial simplifying assumptions.

3. Mechanical Design

The mechanical design has attempted to integrate the efforts of the electrical design and the structural analysis. Figure 15 shows an engineering layout for the maximum gain AIRMAT paraboloid antenna configuration. In this maximum

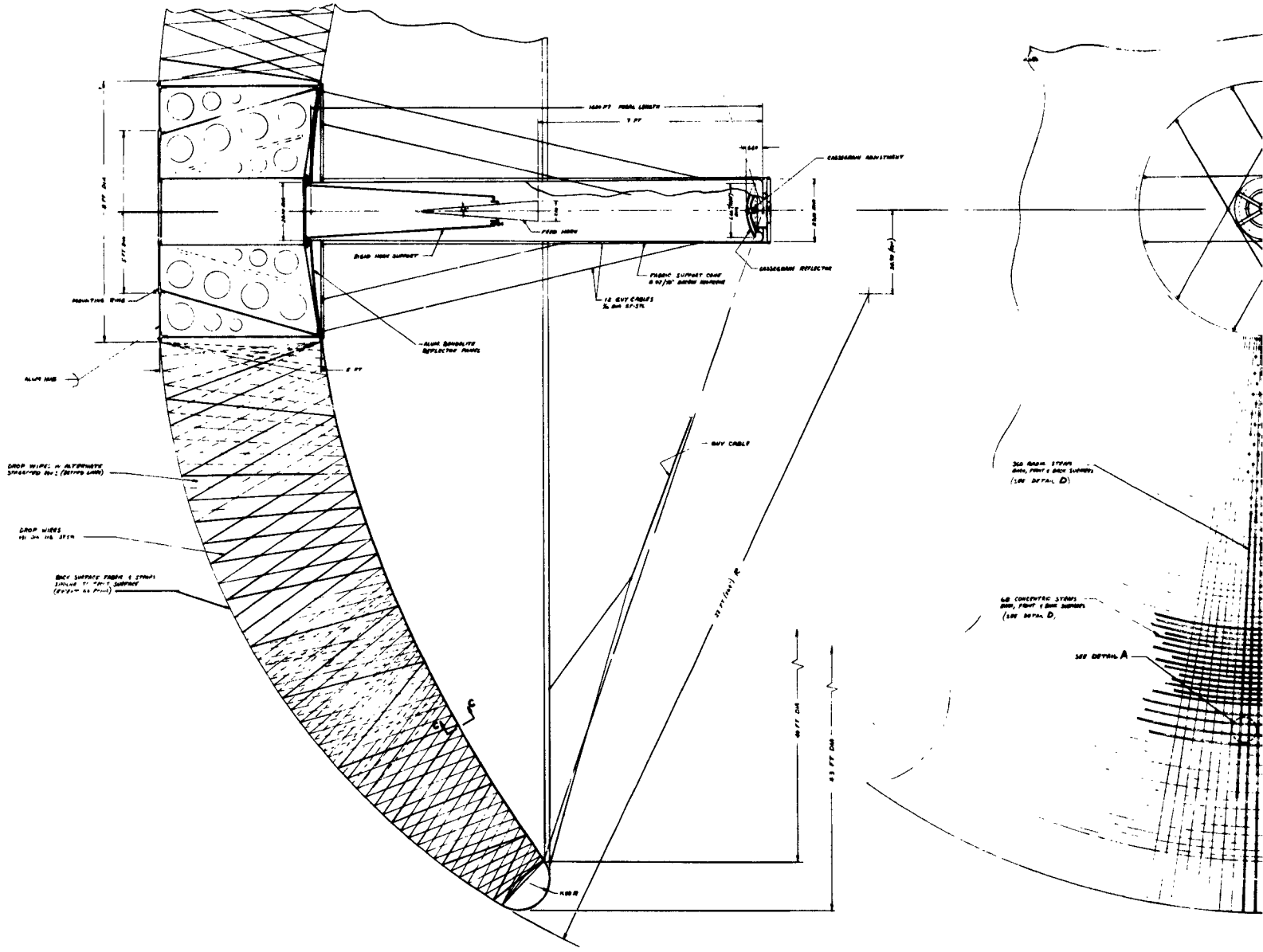
GUY CABLE
SEE DETAIL A

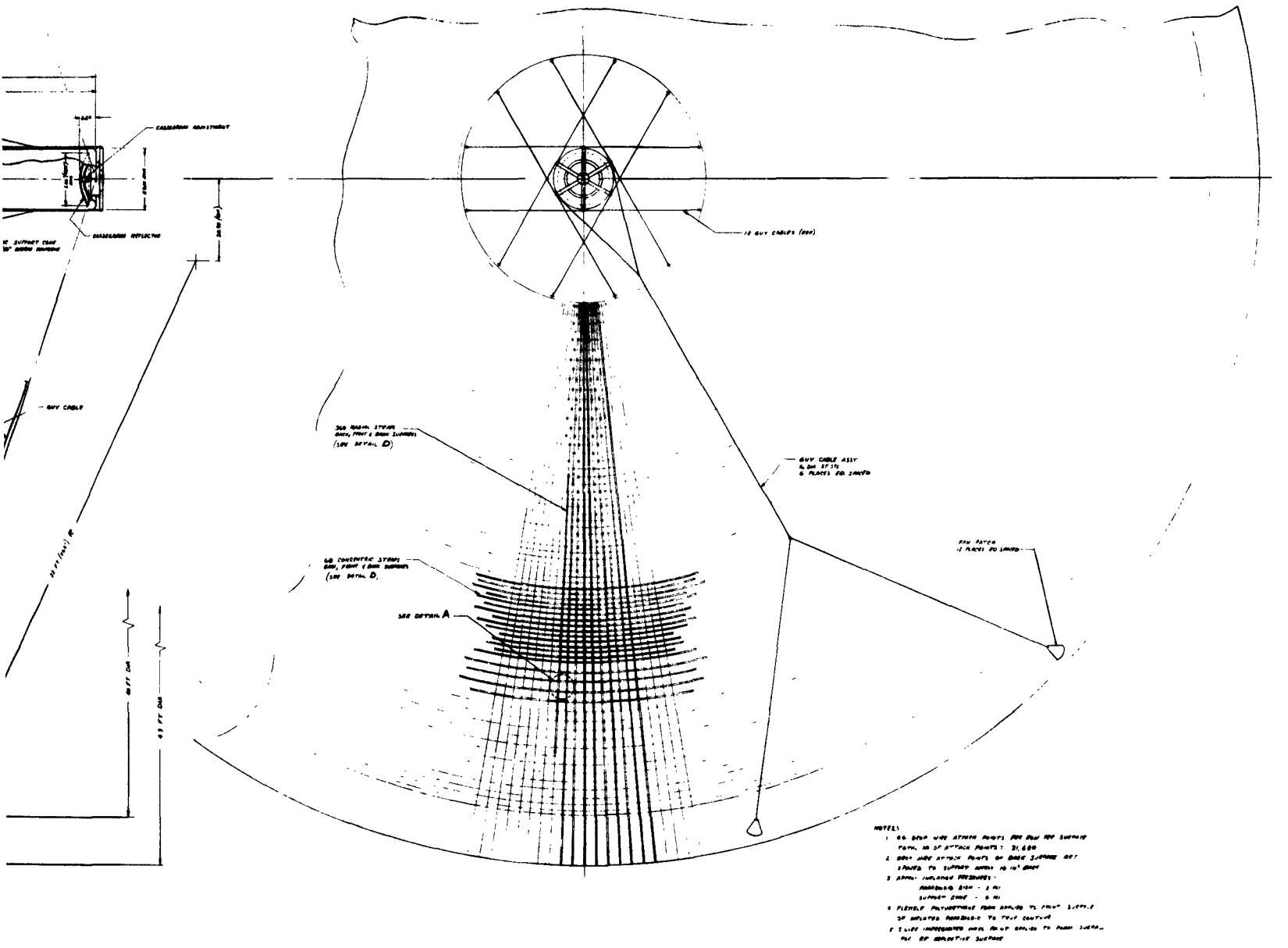

Figure 15 - AIRMAT Paraboloid Antenna (Sheet 1)

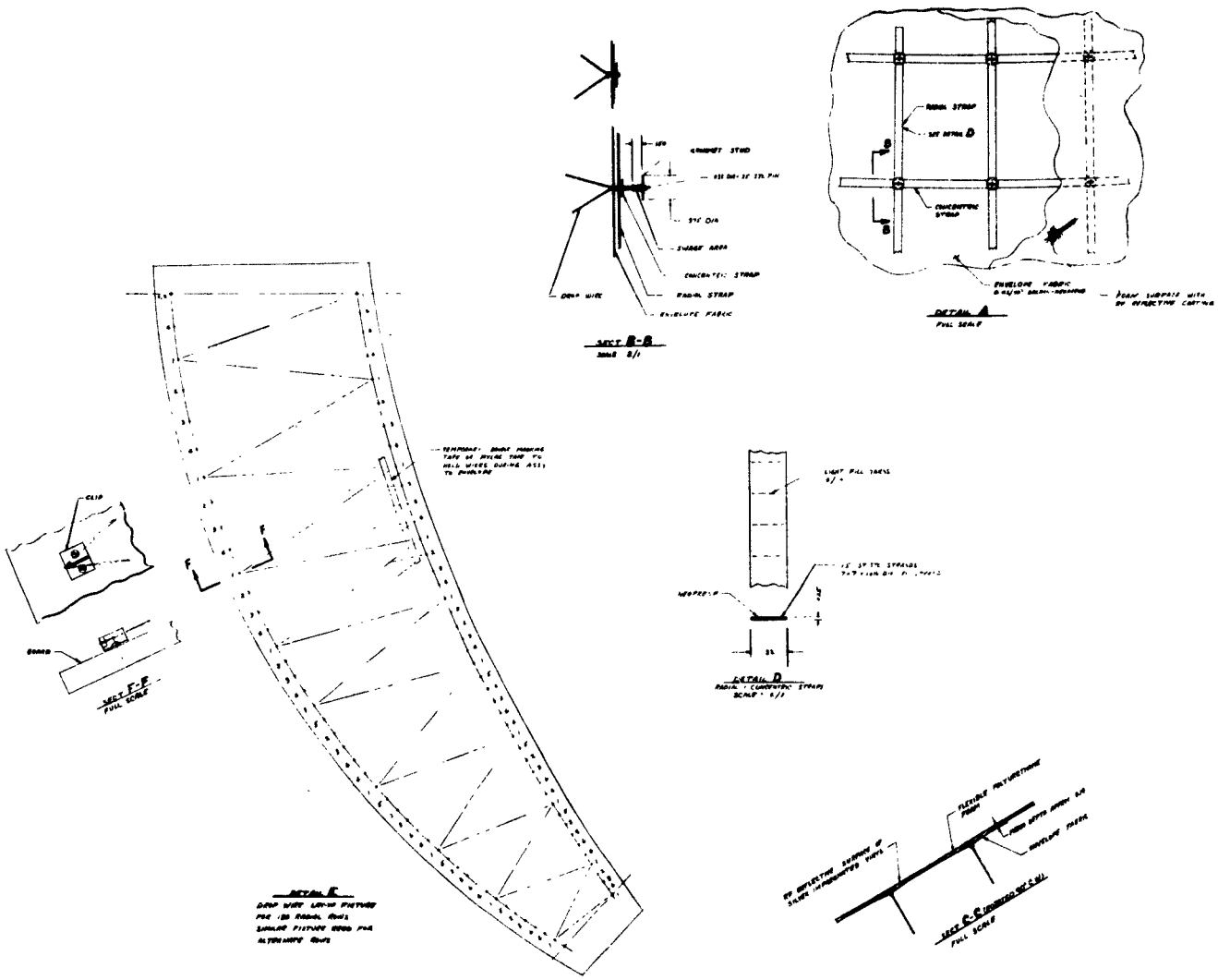

Figure 15 - AIRMAT Paraboloid Antenna (Sheet 2)

gain configuration, the secondary hyperbolic reflector is supported by an inflatable cylinder and by a series of 12 guy cables. The inflated cylinder functions to provide an axial pressure force on the secondary dish assembly, which is reacted by the 12 guy cables anchored to the outer edge of the rigid hub structure. Thus, the cylinder provides only an axial force, and the guy cables serve to orient the dish in focal distance, lateral position, and angular position. Additional cables are also provided and attached to the outer rim of the inflated dish to provide additional support to the secondary dish.

A rough adjustment of the Cassegrain reflector position is made by adjustment of the cable lengths, and a fine adjustment is then made by a separate Cassegrain adjustment as shown in Figure 15.

The feed horn is supported on an adjustable tripod arrangement inside the inflatable cylinder.

The AIRMAT reflector design is basically the same as described in the second quarterly progress report except for some improvement in the drop cord pattern. Figure 15, however, defines further the hub configuration and the related dish and feed horn support and secondary dish attachments.

Figure 15 also shows some detail on the drop cord skin attachments. The drop cord fitting is attached to the skin at the intersections of the concentric straps and the radial straps. The fitting is a swage attachment having a grommet that is bonded to the skin and the straps. The drop cord loop is pushed up through the fitting. A small pin is inserted through the loop to prevent any slippage, and the cable is then swaged to the fitting. A drop cord layout fixture is used to layout the exact length of the cords for a complete radial member.

A second paraboloid antenna configuration, which will probably utilize a more packageable subdish and feed horn configuration and will involve a larger secondary reflector with somewhat greater blockage effects, is being studied.

C. LENTICULAR AIRMAT ANTENNA DESIGN

The lenticular AIRMAT antenna design is also being considered in three basic areas of investigation: electrical design, structural design, and the mechanical design. The over-all design effort has not been completed; however, so far it appears that perhaps a problem may exist with the phase angle variation.

The electrical design has considered the effects of phase angle variation and reduction of gain due to the drop threads and outer structure. Based on the initial assumptions and the resulting calculations, it appears that the use of this antenna may be limited to frequencies below 5000 mc. This problem will be resolved before the completion of Phase IV. Blockage effects of the subdish for this antenna have also been computed. No other critical problems, however, are evident at this time, and perhaps some technique is still available to improve the frequency limitation.

The structural analysis has not yet been completed, but the effort to date has not indicated any problem areas.

The mechanical design also has not indicated any severe problem areas.

1. Electrical Design Considerations

The electrical design for the AIRMAT lenticular antenna was based on 40-foot-diameter Class III Cassegrain antenna.

An f/D (ratio of focal length to aperture size) of 0.35 was selected for the antenna design. With this f/D ratio (assuming that the antenna envelope is a symmetrical double-paraboloid lenticular shape), the focal point is thereby located very near the forward surface that is opposite the reflective surface of the antenna. This f/D selection eliminates the need of additional support structure for the secondary reflector which can then be supported by the opposite side of the lenticular structure.

The secondary reflector dish that was chosen for this design is 39.6 inches (3.3 feet) in diameter. This is greater than the 1.6-foot diameter required for the maximum gain configuration, as was used in the design of the AIRMAT paraboloid antenna.

The electrical characteristics for the AIRMAT paraboloid antenna, with a 10-db illumination taper and a 55 percent efficiency, will have a gain of 59.5 db. Due to blockage, the gain of the lenticular AIRMAT antenna will be 59.38 db instead of the 59.5 without blockage. Figure 9 includes a curve indicating the expected side lobe levels for the lenticular AIRMAT antenna with blockage versus various design side lobe levels without blockage. The degradation in side lobe level resulting from this increase in blockage might be considered negligible as compared to the benefit derived from the increased diameter of the secondary dish, for it permits the location of the feed horn within the hub, rather than in an extended position toward the secondary dish as was done in the case of the AIRMAT paraboloid (see Figure 15). This simplifies the feed horn support and provides better packageability.

The lenticular AIRMAT antenna electrical analysis has been conducted with the following assumptions:

(1) The dielectric constant of the drop threads is 6.1.

(2) The drop threads are uniformly distributed in the lenticular AIRMAT antenna volume.

(3) The volume ratio of drop threads to enclosed air volume in the antenna is 0.000965.

(4) The opaque surface will have a negligible effect on the electrical parameters.

In evaluating the antenna concept in support of continued mechanical

development, the aperture phase distribution appears to be the most critical problem area thus far encountered.

The dielectric constant of the drop threads is 6.1, and the drop threads are considered uniformly distributed throughout the enclosed antenna volume. This assumption allows the use of the following formula to determine the composite permittivity (dielectric constant):

$$\epsilon_c = 1 + \frac{\text{volume of dielectric}}{\text{Total Volume}} \quad (\epsilon_0 - 1)$$

$$= 1 + 0.000965\ (6.1 - 1)$$

$$= 1.00493.$$

This new dielectric constant can be used to determine the phase delay of the energy propagating through the drop threads. Consider the path traveled by the microwave energy as it leaves the Cassegrain subdish. If we consider the drop thread medium that the energy passes through as having a constant dielectric, then, like air, the plane wave front perpendicular to the direction of propagation will contain "in phase" wave energy; but if the dielectric constant changes,the plane wave front will have a varying phase. The maximum permissible variation should be less than 1/16 wave length to ensure negligible effects on the antenna's electrical characteristics.

Figure 16 should aid the reader in interpreting the phase variation due to change in the dielectric medium. A ray of energy travels at the velocity of light along paths from the subdish toward the reflector, where they are reflected back parallel to the axis of the feed. The phase of this energy will be constant in a plane perpendicular to the direction of propagation. The rays of energy in the lenticular AIRMAT antenna will travel the same path, but due to the dielectric, the velocity of propagation will be reduced. This reduction in velocity would not affect the phase of a plane wave front if it were constant for

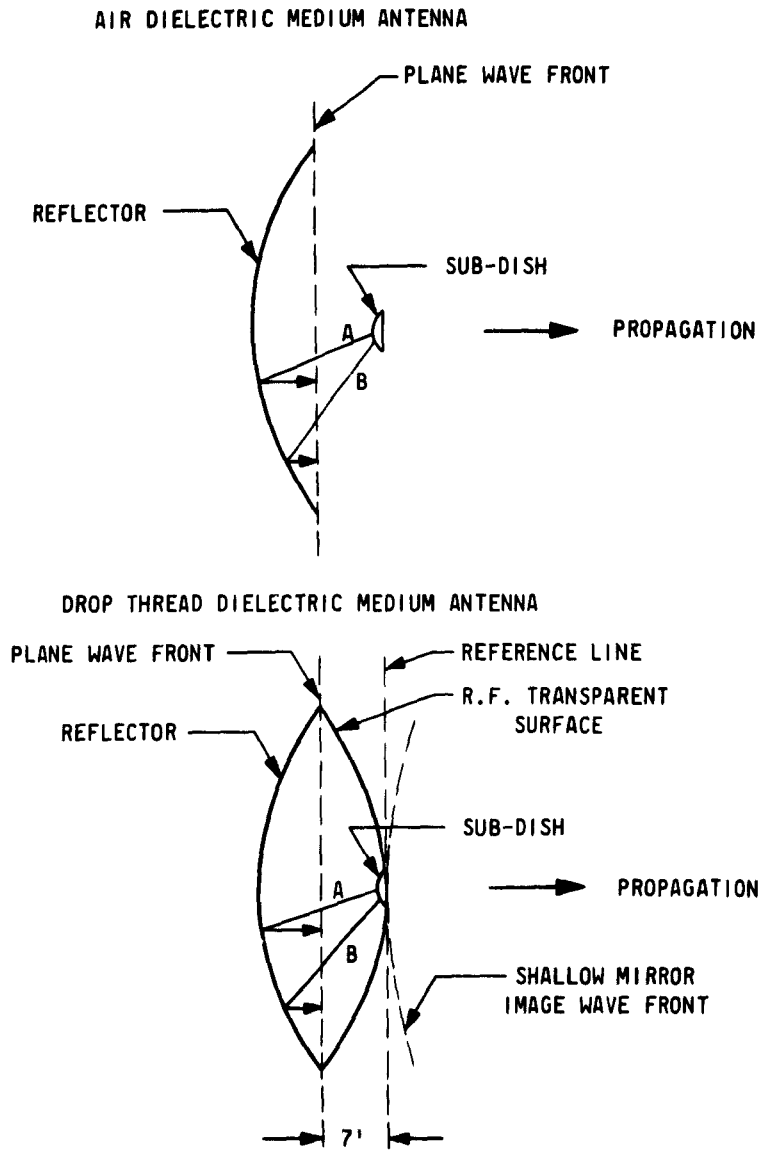

Figure 16 - Schematic Wave Front Comparison between Air and Drop-Thread Dielectric Medium

all possible ray paths. The phase front of a plane perpendicular to the direction of propagation bisecting the antenna is "in phase", but as the wave passes out of the antenna into air, the equal phase front is modified. The equal phase front is no longer a plane, but a shallow mirror image of the paraboloid shape.

To determine the maximum phase deviation of the shallow mirror image, the wave length difference between a ray at the center of the reflector and a ray at the edge of the reflector is determined.

From the relation, propagation velocity

$$= \frac{\text{velocity of light}}{(\text{dielectric constant})^{1/2}} .$$

Determine the wave length of 10 gcs in free space

$$\lambda_0 = \frac{984}{f(\text{mc/sec})} = \frac{984}{10000} \text{ ft} = 0.0984 \text{ ft.}$$

Then the wave length in the dielectric is

$$\lambda_\epsilon = \frac{0.0984 \text{ ft}}{\sqrt{\epsilon_c}}$$

$$= \frac{0.0984 \text{ ft}}{\sqrt{1.0049}}$$

$$= \frac{0.0984}{1.00245} \text{ ft.}$$

The differential phase, $\Delta\phi$, occurs over a distance of 7 feet

$$\Delta\phi = \frac{7 \text{ ft}}{\left(\frac{0.0984}{1.00245}\right) \text{ft}} - \frac{7 \text{ ft}}{0.0984 \text{ ft}} = 0.174 \text{ wave lengths.}$$

Thus, as previously stated, the phase variation should be less than 1/16 wavelengths. This value would cause appreciable degradation of the side lobe level

with slight degradation of gain for a frequency of 10,000 mc. At a frequency lower than 5000 mc the phase variation will be less than 1/16 wavelength and amount to only slight degradation.

The amount of degradation depends upon the magnitude of the gain and side lobes. If the side lobe level had been -26 db, the new side lobe level would be approximately -23 db, a 3-db increase in side lobe level. This example is a result of interpolating the information from a normalized antenna radiation pattern and may contain some inaccuracies. Had the ideal side lobe level been lower, the resultant side lobe level with this phase error would remain at approximately -23 db. The gain would be slightly decreased, but in all cases would be less than 1 db.

2. Structural Analysis of the Lenticular AIRMAT Antenna

a. General. As in the case of the AIRMAT paraboloid antenna, several simplifying assumptions have been made to reduce the over-all effort and for use in expediting the design of this concept. On the other hand, the design criteria has been established to meet the more severe deflection requirements of the 40-foot diameter, Class III antenna. Also, the assumptions made for the analysis in most cases are conservative so that any problem areas can be readily established.

The structural analysis is based on a circular flat plate of constant thickness with the pattern drop threads being constant in either direction. In the actual antenna where the slant drop threads are in radial rows terminated at the hub, the equivalent of this condition can be closely approximated by proper spacing and staggering of the drop thread attachment points to create equal pressure areas.

To date, only the symmetrical loading condition has been investigated. In

this case, the applied forces are from the static weight of the antenna with the antenna in the zenith attitude. For this condition, it has been shown that the deflections are well within the required limits. With this analysis and with the additional information that can be extrapolated from the AIRMAT paraboloid analysis, it has been adequate for the additional preliminary design studies thus far. However, some additional work will be necessary to finally prove out this structural concept.

The continuation of Phase IV during the next quarter will consider this effort further.

b. Analysis Approach. A schematic diagram of the lenticular AIRMAT antenna is shown in Figure 17. In this analysis, both the stresses and maximum deflections are checked.

If the theory of Reference 3 applies and m = n, the load in a drop thread is given by Equation 55:

$$T_d = \frac{p}{2n^2 \cos\theta} \pm \frac{v}{2\pi rn \cos\theta} \quad . \tag{55}$$

The first term in Equation 55 is due to the internal pressure, and the second term is due to the applied shear stress. If

$$\frac{v}{2\pi rn \cos\theta} > \frac{p}{2n^2 \cos\theta} \quad ,$$

one set of drop threads will become slack, resulting in collapse of the AIRMAT panel. Thus,

$$\frac{p}{n} \geq \frac{v}{\pi r} \quad \text{or} \quad p \geq (nv)/\pi r). \tag{56}$$

From Reference 4, the maximum bending stresses in circular plates are given by Equation 57:

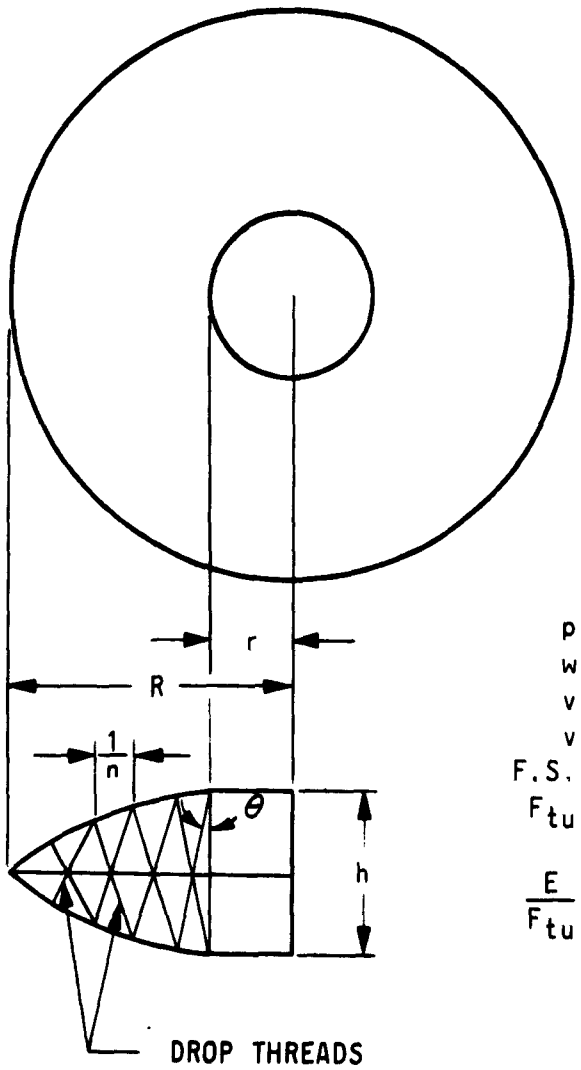

p = INTERNAL PRESSURE
w = UNIFORM LOAD PER UNIT AREA
v = TOTAL LOAD
$v = w\pi R^2$
F.S. = FACTOR OF SAFETY
F_{tu} = ULTIMATE TENSILE STRESS OF FABRIC
$\frac{E}{F_{tu}}$ - STIFFNESS - STRENGTH RATIO OF MATERIAL

$$\approx \frac{6000000\ PSI}{100000\ PSI} \approx 60$$

Figure 17 - Schematic Diagram of AIRMAT Lens Antenna

$$\sigma_{max} = \pm\ k \frac{wR^2}{h^2} \text{ (for a solid cross section)} \tag{57}$$

Modifying Equation 57 for an AIRMAT cross section,

$$\sigma_{max} = \pm\ k \frac{wR^2}{h^2} \left[\frac{(1/12)(h^3)}{(h^2/2)} \right] = k \frac{kwR^2}{6h} \quad .$$

To prevent wrinkling,

$$\frac{kwR^2}{6h} > p(h/2),$$

or

$$p = \frac{kwR^2}{3h^2} \tag{58}$$

where k = 5.10 for the boundary conditions of this study.

Thus, the required internal pressure can be selected using Equations 56 and 58.

The effective shear modulus of an AIRMAT panel with inclined drop thread is given by the following equation (Reference 3):

$$(Gh)_{eff} = ph + 2n^2 h\, A_d E_d \sin^2 \theta \cos \theta \tag{59}$$

where

$$A_d E_d = FS \times T_d \times \frac{E}{F_{tu}} \quad . \tag{60}$$

The maximum deflection due to shear is given by Equation 61:

$$(Y_{max})_{shear} = \frac{w}{2(Gh)_{eff}} \left[R^2 \log (R/r) - \left(\frac{R^2 - r^2}{2} \right) \right] . \tag{61}$$

From Reference 4, the maximum deflection due to bending in a circular plate is

$$w_{max} = k_1 \frac{wR^4}{Eh^3} \quad . \tag{62}$$

Applying Equation 62 to an AIRMAT cross section,

$$(w_{max})_{bending} = k_1 \frac{wR^4}{Eh^3} \frac{(1/12)(h^3)}{h^2/2} = k_1 \frac{wR^4}{6Eh^2} \tag{63}$$

where

$$E = \left(\frac{E}{F_{tu}}\right) \quad F_{tu} = \left(\frac{E}{F_{tu}}\right) (ph)\,(FS) \tag{64}$$

and

k_1 = 1.31 for the boundary conditions of this study.

The particular antenna considered in this study has the following dimensions:

h = 14.0 ft,

R = 20 ft,

γ = 4 ft,

v = 1500 lb (1 g),

$w = \frac{1500}{\pi R^2} = 0.00830$ lb/in.^{2},

and

n = 2 drop threads per foot.

A fiberglass material will be used in which

$E/F_{tu} \cong 60$

and

FS = 4.

As between Equations 56 and 58, the necessary governing internal pressure is 239 psf (from Equation 56).

From Equation 55,

$T_d = 59.7/\cos\theta$.

From Equation 60,

$$A_d E_d = 240 T_d = \frac{14350}{\cos \theta} .$$

Substituting in Equation 59 and 61,

$$(Y_{max})_{shear} = \frac{270}{(Gh)_{eff}} = \frac{270}{3350 + 1.6 \times 10^6 \sin^2 \theta} .$$

From Equation 64,

$$E = 402,000 \text{ lb/ft.}$$

Whence from Equation 63,

$$(w_{max})_{bending} = 0.00053 \text{ ft.}$$

The total maximum deflection is

$$(w_{max})_{shear} + (w_{max})_{bending}$$

$$= \frac{270}{3350 + 1.6 \sin^2 \theta} + 0.00053.$$

If $\theta = 30^o$, the total maximum deflection = 0.00120 feet, which is well within the required tolerances. The required drop thread area is

$$A_d = \frac{T_d \, FS}{F_{tu}} = \frac{(59.7/\cos 30^o)(4)}{100,000} = \underline{\underline{2.76 \times 10^{-3} \text{ in.}^2}}$$

The required face sheet strength is

$$(F_{tu})_{cloth} = \left[\frac{ph}{2} + \frac{kwR^2}{h^2}\right] \left[FS\right] \cong \underline{\underline{560 \text{ lb/in.}}}$$

3. Mechanical Design

The mechanical design of the full-scale Lenticular antenna, shown in preliminary form Figure 18, has attempted to integrate the electrical design

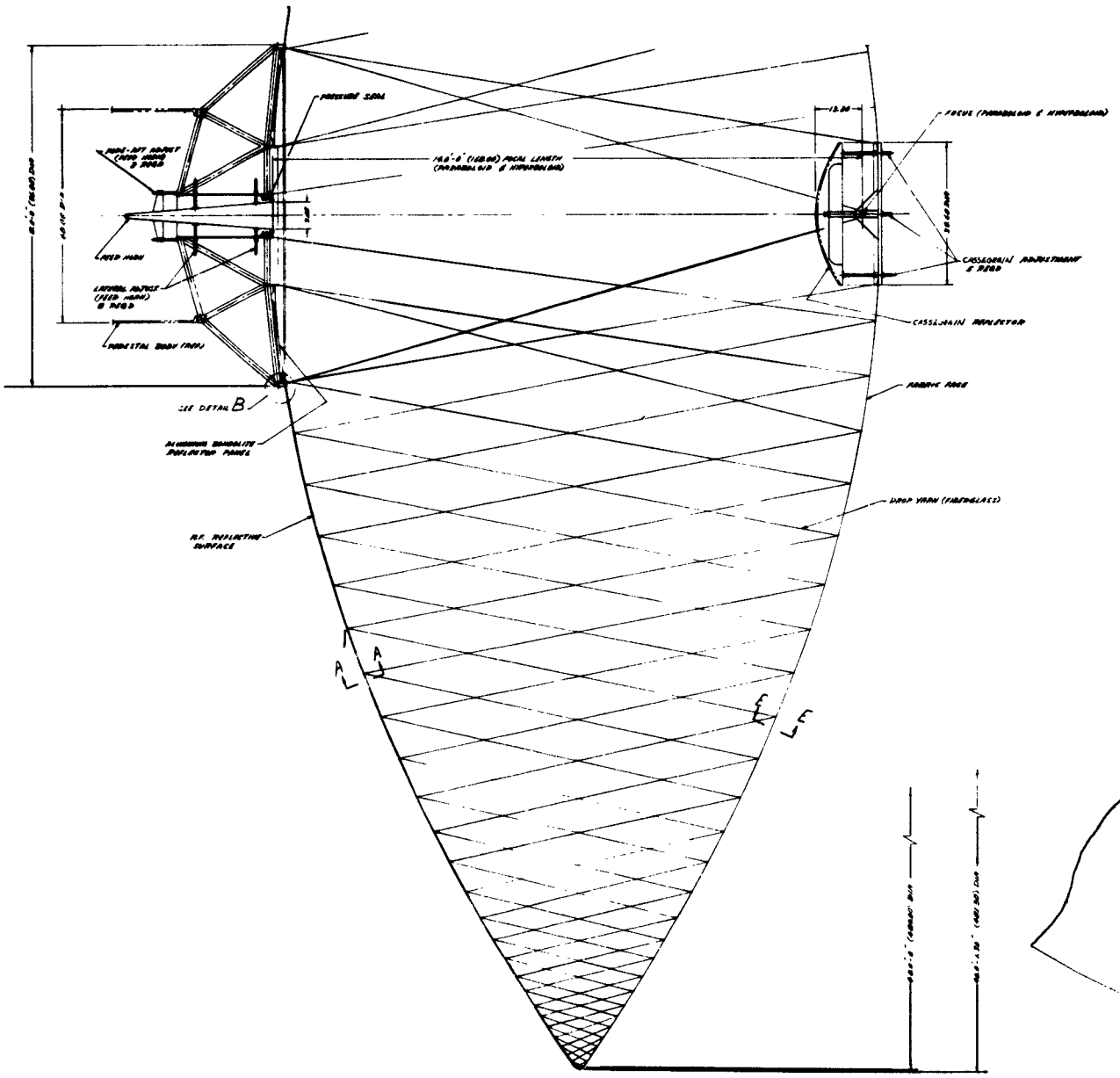
PRESSURE SEAL
FOCUS (PARABOLOID & HYPERBOLOID)
CASSEGRAIN SUBREFLECTOR & ROOD
CASSEGRAIN PROJECTOR
FENDING RING
SEE DETAIL B
DROP YARN (FIBREGLASS)
R.F. REFLECTIVE SURFACE

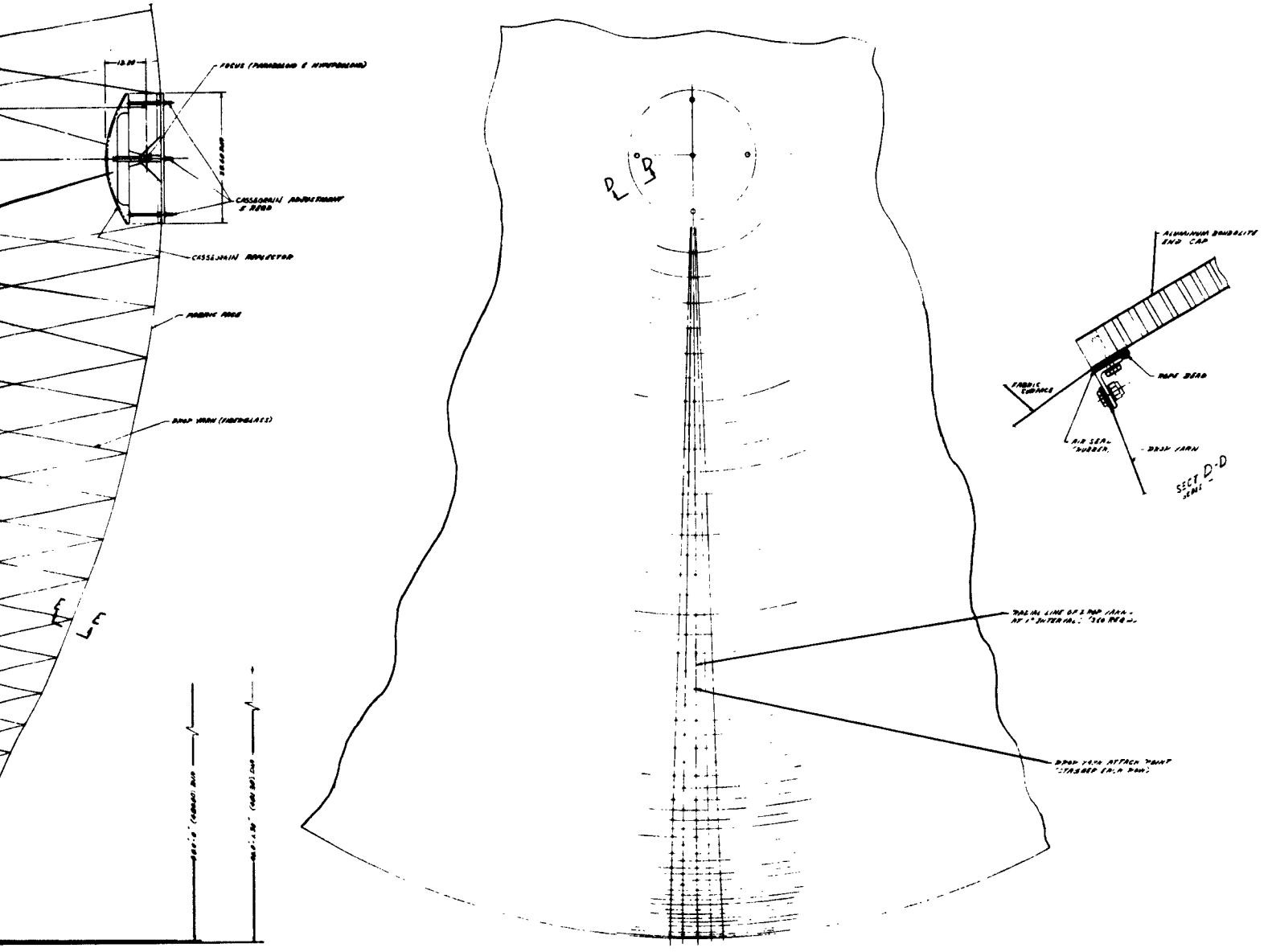

Figure 18 - Lenticular AIRMAT Antenna (Sheet 1)

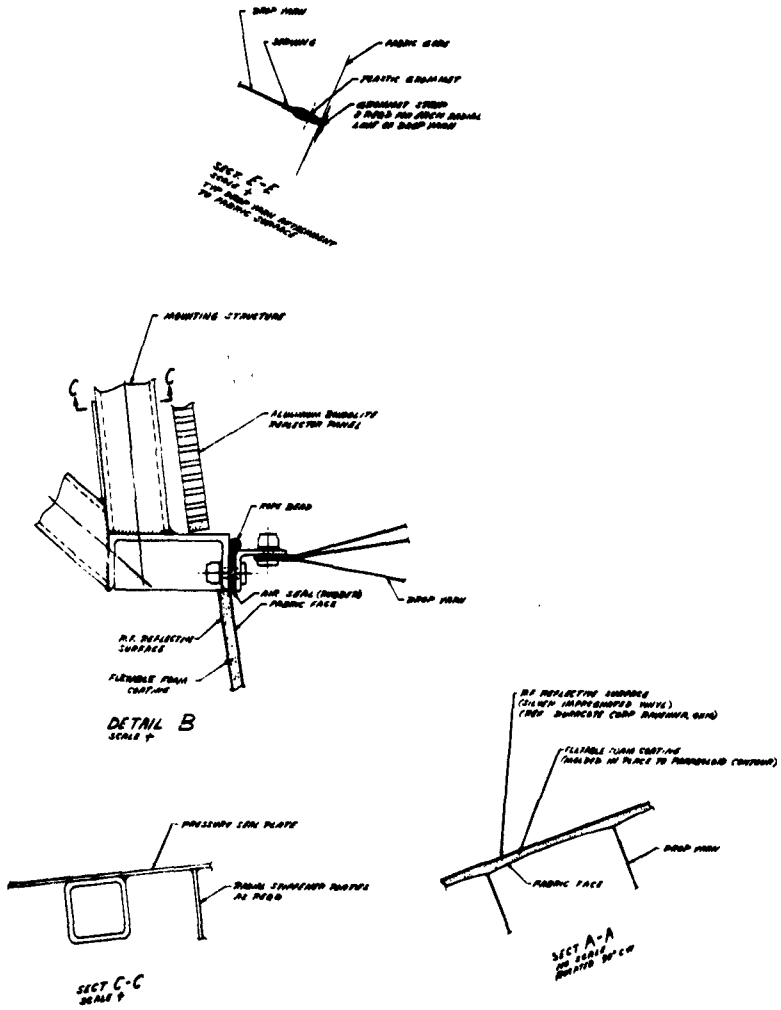

Figure 18 - Lenticular AIRMAT Antenna (Sheet 2)

considerations and the structural analysis. Neoprene-coated fiberglass fabric and fiberglass drop cords were selected for the structure to obtain maximum stability and rigidity.

The configuration is essentially the same as the concept shown in Figure 34 of the second quarterly report, with the exception of the secondary dish support. The rigid fiberglass cylinder secondary dish support has been eliminated because of the r-f transmission problems it would create. The dish is supported in an adjustable manner from a rigid circular BONDOLITE* plate mounted directly to and supported by the envelope fabric. The drop cords, which support the circular plate to the outer rim of the rigid hub structure, are arranged to give rigidity to the secondary dish support in the axial and lateral directions and in angular position.

The feed horn is mounted within the hub with its aperture at the apex of the paraboloid. A flexible pressure seal is provided between the horn aperture and the hub structure to allow for horn adjustment. The hub structure shown is a tubular-space frame-type structure with a 5-foot diameter mounting ring for mounting to the pedestal. Inflation pressure is retained at the hub by the rigid reflector panel in the outer portion and by an aluminum bulkhead attached to the feed horn support tube.

Figure 18 shows the arrangement of the drop cords, which are arranged in radial rows, each row terminating at the hub area. The drop cord attachment points are carefully spaced in the rows and staggered from row to row to achieve approximately equal pressure loading on all cords and to achieve approximately the same slant angle on all cords. The attachment of the drop cords to the fabric envelope is made by lacing the cords into a fabric "T" section which forms a part of the seam between gores. A fabric "T" is installed

*TM, Goodyear Aircraft Corporation, Akron 15, Ohio

for each row of drop cords. The exact length of each drop cord is predetermined by use of a layout fixture onto which each radial row of cords is laced before assembly into the envelope.

D. REFLECTOR CONTOUR DEVELOPMENT

1. General

To develop an accurately contoured r-f reflective surface, a test program has been planned to aid in determining the materials and fabrication techniques that can be used to form the proper contour and provide an r-f reflective surface. A series of model testing is planned, each of which is progressively more difficult to perform. Three types of AIRMAT will be used: flat AIRMAT samples, a single-contoured AIRMAT panel, and finally the five-foot-diameter antenna models. To date, however, the only tests that have been conducted are some very preliminary foaming tests on the flat AIRMAT samples.

This work effort has been divided into two areas which incorporate two separate development areas:

(1) Contour foaming development
(2) R-F reflective surface development

2. Foaming Contour Development

As mentioned above, the only tests performed so far have been some very preliminary foaming on flat AIRMAT panels. The objectives of the tests were to observe the physical characteristics of the latex foam during the foaming process and to examine different foaming techniques. The tests were also to establish foam adherance to the AIRMAT and to check out the latex foam resistance to permanent creasing when folded. In subsequent testing, however, an AIRMAT panel support fixture will be used to also develop a highly accurate flat surface on the foam.

The test procedure and some of the results of the tests are given in the following paragraphs.

a. Foaming Test Procedure. A latex foam of approximately 13 lb/ft^3 density was applied to four AIRMAT panels approximately 18 x 18 inches square and one inch thick. The foam was then swept over the AIRMAT panel, providing a depth of foam varying from 1/2-inch thickness to about 1/8 inch. On some panels, an adhesive was used to check the difference in adherance of the foam. After being allowed to "jell" for a few minutes, a glass plate was placed on the foam surface and a load was applied to compress the uncured foam. Then, after allowing the foam to set up for an additional length of time, the glass plate was pealed off and the test panel was placed in a curing oven at 212^{o}F to complete the curing cycle. Figure 19 is a photo of some foamed AIRMAT test samples. The surface shown on the right has an experimental reflective coating that was subjected to flexure tests. Further tests will be conducted, and the results will be included in the subsequent monthly letter report.

b. Characteristics of Foamed Airmat Samples. These preliminary test samples exhibited the following characteristics of the latex foamed surface:

(1) Excellent resistance to creasing after repeated folding.
(2) Good adherance of foam to AIRMAT panel.
(3) Surface porosity and open-celled foam structure.
(4) Tendency of foam surface to form a meniscus during jell.

In folding the cured latex foam AIRMAT panel, no permanent creasing was observed in the foam even when held in a folded position for some time.

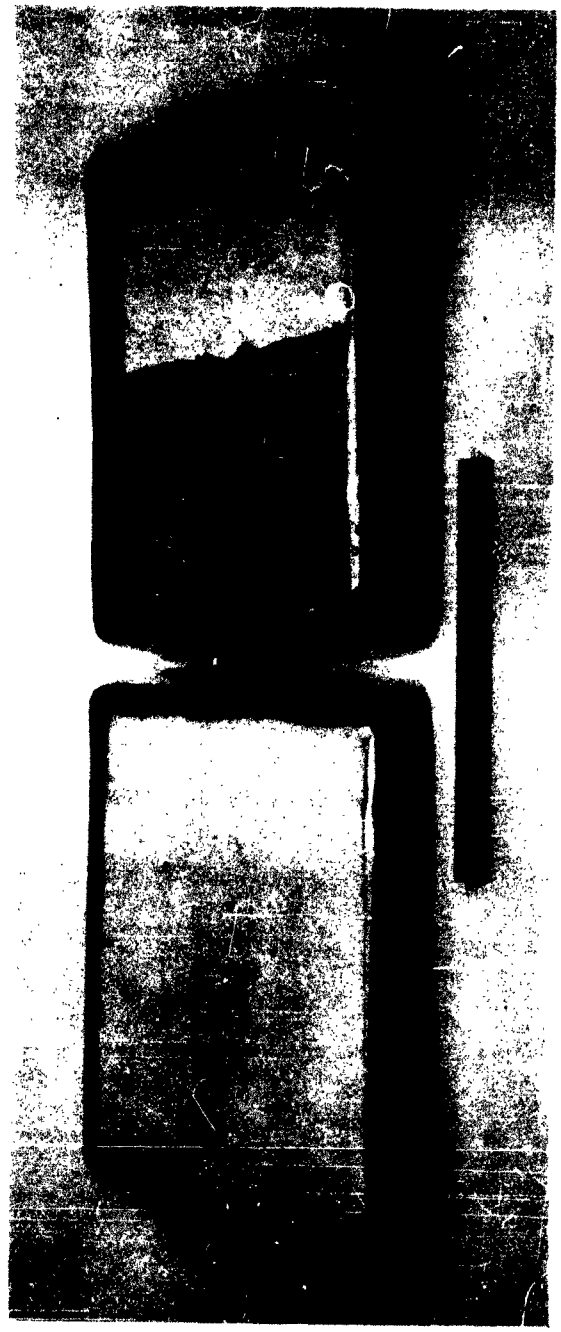

Figure 19 - Flat AIRMAT Samples for Foamed Surface Development

More severe tests will be given, however, in subsequent testing of other AIRMAT panels.

It was noticed that the foam bonded quite readily to the AIRMAT surface with or without the use of an adhesive. Some improvement in adhesion was noted when the adhesive was used.

The surface porosity and the open-celled structure characteristics of latex foam would allow the surface to be moisture absorbant. This minor problem, however, can be alleviated by application of a sealer or film. In fact, some of the planned tests, which will be explained later, will utilize a film that already contains the r-f reflective material. These possibilities are discussed in more detail later in this section. It should be also noted that when the test batch of latex foam was whipped, larger bubbles formed than would be expected in a production batch processed in specialized equipment. In any case, the bubbles are not large enough to degrade the antenna performance.

The tendency of a meniscus to form is the result of chemical action within the foam during the jelling process. This characteristic, however, does not affect the molding process, since the foaming of the final contour does not occur until after the jelling process. It must be taken into account, though, in planning the final foaming procedure. One additional test panel was foamed using polyurethane foam instead of latex. In this case the density of the foam was approximately 2 lb/ft^3.

To foam the panel, the unexpanded foam mixture was poured over a flat plate using a polyethylene film as a separator. The AIRMAT was then lightly pressed on the foam as it expanded.

As a result of this test, it was noted that the foam generates a significant pressure while expanding, and the depth of the foam on the AIRMAT panel must be controlled by providing a foaming tool to uniformly distribute the foaming pressures without deflecting the AIRMAT structure. The support for the back side of the AIRMAT must exactly conform to its contour. Any nonconformity in this support will result in an equal foam surface deviation when released from the mold and allowed to spring back. It was also noticed that gas bubbles could form on the surface of the foam and leave imperfections in the foam surface, if the tool is not porous to allow for the gas leakage.

In comparing the two types of foams, the following physical characteristics have been noted:

(1) The latex foams exhibit the better crease resistance. It is anticipated that the difference will become more obvious at the lower temperatures. This fact does not necessarily rule out the polyurethane foam, since much improvement can be accomplished through change in formulation.

(2) The polyurethane foam has a closed surface requiring no sealing process as will be necessary with the latex foam. The polyurethane will have a surface finish equal to that of the mold used against it.

(3) Both types of foam can be cured at ambient temperature, but polyurethane foam can be oven-cured in a shorter time if time becomes an important factor.

The cured weight of polyurethane foam is approximately 1/6 that of the latex foam. On antennas of considerable size, this weight difference may become a substantial advantage.

(4) Polyurethane foam tends to blow itself out when forced to enter small cavities, more so than the latex foam, which appeared to undergo little change in cell size throughout varying thickness. Again, formulation can do much to correct this deficiency in the polyurethane foam. Some sample of foamed pads using a "35P" formulation had cross section thicknesses varying from 0.5 inch feathered to nothing without excessive blowing. This can also be attributed to proper mold design.

As yet, it appears that neither foam has demonstrated any superior advantage over the other, nor has either shown a disadvantage that would preclude its use.

3. Subsequent Reflector Surface Development

Further foam testing with the flat AIRMAT panels will be accomplished in an adjustable mold made especially for that purpose. The adjustability feature will permit varying thicknesses of foam. Two different materials are to be used as the contour-conforming backup support. The first is the use of sand, which has the advantage of being reusable for a number of successive AIRMAT panels. The second material is a rigid polyurethane foam. The latter has the disadvantage of requiring a separate support for each individual panel; however, it will probably be the most feasible technique for foaming the larger single-contoured AIRMAT panel and the 5-foot-diameter test models.

When using the rigid foam, it is poured directly on the reverse side of the AIRMAT and allowed to harden. A flat surface is then obtained on this rigid foam by merely sawing off a small portion of excess foam.

4. R-F Reflective Surface Development

As a follow-on test, the latex- and polyurethane-foamed AIRMAT panels will

be painted with three coats of a silver-impregnated vinyl paint. These panels will then be tested for r-f reflectance. The results of this testing will be presented in the March monthly letter report.

The Phase IV effort will also investigate other techniques utilizing a film in addition to the r-f reflective paint. The other techniques to be investigated will include:

(a) Heat-forming a film-aluminum-foil laminate over a male parabolic tool by stretching and heating.
(b) Heat forming a film laminate while forming it against a female mold by vacuum.
(c) Spraying with film and reflective material on parabolic tool.

In all the above techniques, after the r-f reflective film has been formed, it is to remain in place on the mold and the foaming accomplished as previously described so that the foam adheres to the film as well as to the AIRMAT. The film in some cases may require that it first be covered with an adhesive when a latex foam is to be used. No adhesive requirement is anticipated with the various polyurethane foams.

E. ADVANCED AIRMAT DESIGN APPROACH

In previous reports of this study, methods and techniques of fabricating the AIRMAT antennas have been discussed. The evolution of the concept has progressed from constant thickness normal drop-thread AIRMAT to slanted drop-cord AIRMAT parabolic dishes having single-contour sections with a tapered cross-sectional thickness. However, although each design feature represents a logical advance in the state-of-the-art in loom-weaving of AIRMAT, each of these features would represent development of new loom-weaving techniques. For this reason, most of the suggested fabrication techniques have been based on hand-weaving the slanted drop-thread antenna dishes.

These slanted drop-thread arrangements provide a satisfactory means of achieving an AIRMAT structure which, as determined by the preliminary analysis, will maintain the antenna contour within the desired limits. The fabrication of these structures can be accomplished without an excessive amount of tooling cost, and the over-all fabrication cost of the antennas does not appear to be excessive. However, in the interest of improving the design still further, and with the possibility of making a reduction in fabrication costs with comparable weight and packaging bulk, the following new structural concept may offer a possible improvement over the previous designs.

The improvement suggested for the antenna designs is to replace the rows of widely spaced slanted drop threads with continuous shear webs having threads spaced closely together. This construction would be quite similar to that used in the construction of the models that will be discussed in Section IV. The main difference is that the fabrics required for the webs would be a stiffer material to provide better rigidity and dimensional control.

The web would be fabricated in a manner that is similar to the radial row of widely spaced slanted drop threads, except that the spacing is reduced. Thus, the web becomes a two-directional cloth with the direction of the two sets of threads arranged at an optimum angle with respect to each other.

Attachment of the webs to the surface fabric is accomplished by use of a woven fabric "Y" member which, in effect, makes a "foot" on the web to attach to the surface fabric (see Figure 20). Heavy cords are integrated with "Y" member at its intersection to become the radial tension member (or cap) of the radial beam structure. This member takes the place of the radial straps in the previous designs.

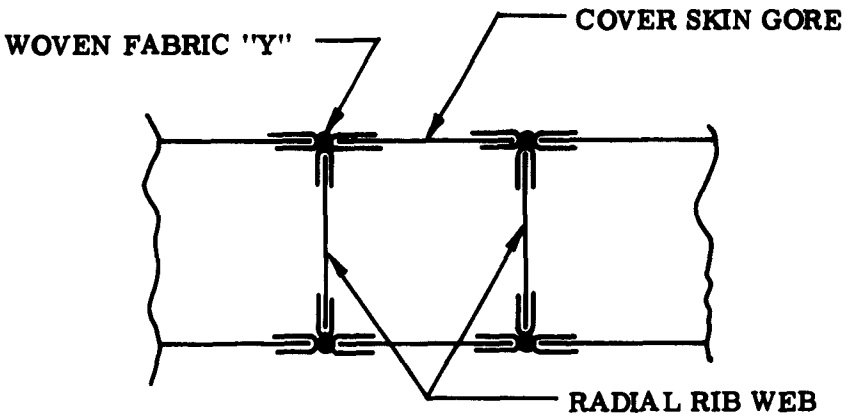

Figure 20 - Schematic of Inflatable Web Structure

Some basic features of the continuous-web concept are as follows:

(1) It appears to function in all respects as well as any previous concept.

(2) The continuous attachment of the web to the surface fabric eliminates the stress concentrations that occur in the previous design at the drop cord attachment points. In addition, the concentric straps are no longer required to transfer the drop cord load to the fabric.

(3) Fabrication is simplified for several reasons. They include:
(a) The concept uses a web patterned from fabric instead of hand-weaving the slanted drop cords.

(b) Continuous bonding of web instead of individual point attachments.

(c) No need to handle large portions of surface envelope as in previous concepts, since the narrow surface gores are progressively attached to the webs, requiring a minimum of tooling and fabric handling.

(4) Because of the elimination of the concentric straps, the weight would likely be decreased and the package bulk may also be improved.

In Section IV, which covers the antenna models, this concept will be discussed further. For the purpose of the models, the fabric-web concept offered not only structural benefits of previous AIRMAT concept but also an economic advantage.

PART 4 - FACTUAL DATA

SECTION IV - PHASE V - MODEL DESIGN AND FABRICATION OF GROUND-BASED TRACKING ANTENNA

A. GENERAL

This phase of the program was planned to design and fabricate antenna models to simulate the construction of the full-scale AIRMAT paraboloid and lenticular AIRMAT antennas. Several benefits are to be gained from this model phase of the program. Some of these benefits include:

(1) Demonstration of the feasibility of this new AIRMAT concept to form the required contour.

(2) Proof of the structural integrity of the AIRMAT utilizing the new technique to develop shear stiffness.

(3) Development of AIRMAT fabrication techniques.

(4) Development of surface foaming techniques.

(5) Development of r-f reflective surface.

(6) Determination of the packaging methods for the inflatable antennas.

B. SINGLE-CONTOURED AIRMAT MODEL

Before attempting to design and build the two scale models, a simpler model was designed and built to determine the most economical model fabrication techniques and to develop the technique for use in the 5-foot-diameter model.

This model, shown in Figures 21 and 22, simulates a panel of the AIRMAT paraboloid. The only differences are that it has a single-curvature surface and the fabric webs, which are used instead of diagonal drop threads, are arranged in parallel rows, rather than radiating from a central hub. The most important function that this model served was the development of a means of simulating the radial rows of slanted drop threads in a way which would be most economical to build and yet be satisfactory in performing the other functions of the model. Methods of slanted drop threads installation similar to the full-scale design were investigated, and workable techniques were conceived. However, because of the small size of the model, it was decided that the fabric web panel construction would be easier and more economical to build than the slant drop-thread arrangement. Good similitude of the full-scale item is difficult to achieve in any scale model of a fabric structure, and it was recognized that the fabric web construction would create a greater penalty in weight and bulk, but these penalties were considered to be outweighed by the economy of construction.

Figures 23 and 24 show different views of the model during fabrication. The success of this model was quite evident after completion. The surface contour of the model was held very close to the planned contour, and no noticeable contour deviations showed up when the internal pressure was varied. This model will also be used during the next quarter in a surface foaming test that will form an accurate r-f reflective surface on the model. The technique that will be used here was explained in the section on the reflector contour development.

C. CONTRACTUAL DEMONSTRATION MODEL DESIGN

The size and contour selected for both antenna models, the AIRMAT paraboloid and the lenticular AIRMAT, are based on an existing parabolic male tool

Figure 21 - Parabolic AIRMAT Panel (Edge View)

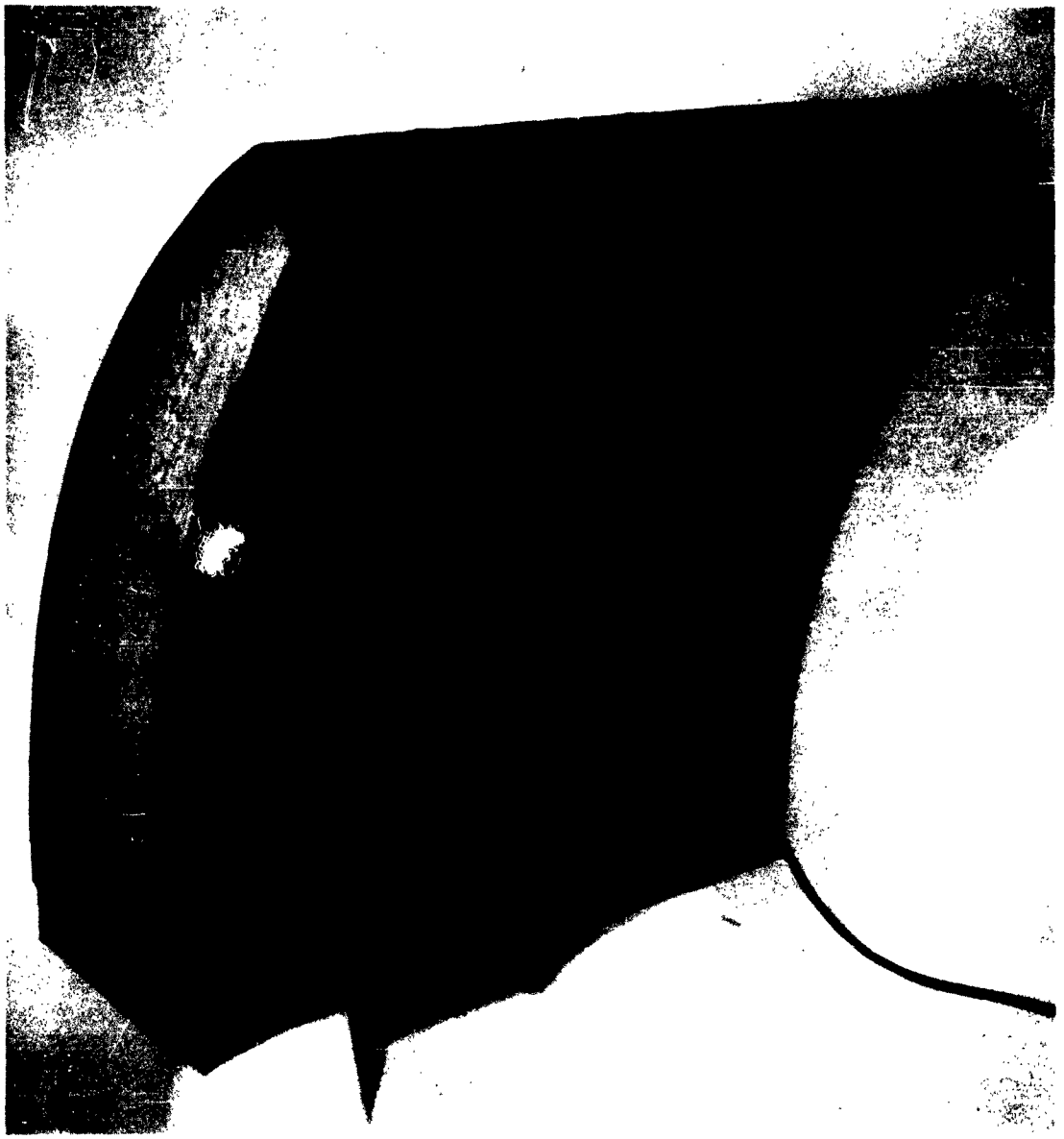

Figure 22 - Parabolic AIRMAT Panel (3/4 Front View)

Figure 23 - View of Model Hub End Showing Fabric Webs (before Hub Was Attached)

Figure 24 - Reverse Side of Model during Fabrication (with Contour Forms in Place)

which will be used to form the final reflector surface contour. This tool is a 5-foot-diameter paraboloid having an f/D (ratio of focal length to aperture size) of 0.30. Its 5-foot diameter is a convenient size, and the f/D ratio was considered satisfactory for the purpose of the models. However, this f/D ratio makes a somewhat deeper paraboloid than the f/D ratio of 0.35 used for the full-scale antenna design. This tool will be used in forming a thin layer of flexible foam onto the inflated parabolic dish to fill in the AIRMAT contour deviations and to provide a highly accurate surface for the r-f reflective paint and film application. The foaming technique was explained in the section covering the reflective surface contour development.

In addition, a female tool must be made to form a similar accurate contour for the lenticular antenna model. A plaster splash will be taken from the available male tool.

Both models are being designed to have construction similar to the preliminary single-contour AIRMAT model using the fabric webs instead of slanted drop cords. With this construction, very simple tooling is required for the fabrication of the model. The only tooling required to fabricate the inflated fabric portion of the model consists of several wood templates cut to the contour of the webs and a metal template of the gore pattern. The method of fabrication used for the models will be similar to that used for the single-contoured AIRMAT parabola.

D. MODEL FABRICATION

The fabrication of the AIRMAT paraboloid antenna model will be initiated during March 1963, and the extent of progress will be reported in the monthly letter report.

PART 5 - CONCLUSIONS

The third quarter effort of the advanced antenna study program has been mainly on the detailed study and analysis of the AIRMAT paraboloid antenna and the lenticular AIRMAT antenna. Some effort has also been expended on the initiation of the Phase V model design in an attempt to provide additional time for design, fabrication, and testing of the antenna models.

During the past quarter, the following conclusions have been established for the ground-based tracking antenna studies:

(1) Additional electrical, structural, and mechanical investigation has further substantiated the potential of the AIRMAT paraboloid antenna concept.

(2) A preliminary model of an AIRMAT paraboloid section has been fabricated, with the model holding tolerances within expected accuracies.

(3) Investigation of foamed r-f reflector surface has involved several techniques of developing this surface. The best concept is yet to be established.

(4) Indications are that the lenticular AIRMAT antenna concept may be best limited to frequencies below 5000 mc due to an excessive phase angle variation caused by the drop-thread dielectric medium.

(5) AIRMAT fabricated with radial webs instead of radial rows of slanted drop cords appear to be functionally as good as any other concept, while still offering comparable weights and packaging bulk.

The following general conclusion can be made in regard to space vehicle antennas: based on the structural, thermal, and dynamic studies performed to date on the Swirlabola antenna, the design appears compatible with space system parameters.

PART 6 - PROGRAM FOR NEXT REPORTING PERIOD

The next reporting period will cover the period from 1 March 1963 to the completion of the program and will be reported in the final report. Phase IV, Detail Study and Analysis, and Phase V, Model Design and Fabrication, will be completed during this period.

The space system antenna study will complete the detail study and analysis of the solid-panel Swirlabola antenna and the design, fabrication, and evaluation of the scale model for this antenna. The model will be tested to demonstrate concept feasibility, packaging and deployment capability, and contour accuracy. Modifications deemed desirable as a result of fabrication and evaluation of the model will be integrated into the full-scale design concept.

In completing Phase IV of the program, the ground-based antenna studies will be directed toward resolving basically the technical problems of developing an accurate r-f reflective foam surface on the inflatable antenna concepts. Further consideration will also be given the structural and electrical characteristics of the lenticular AIRMAT antenna and some electrical evaluation for the AIRMAT paraboloid antenna.

The latter portion of the program will be finalized by completing the fabrication and evaluation of the inflatable antenna models and by submitting the final report for the program.

PART 7 - IDENTIFICATION OF PERSONNEL

Table VI lists the manhour totals used by key personnel for the third quarter.

Table VI - Manhour Breakdown for Third Quarter

PERSONNEL		THIRD QUARTER TOTAL
Name	Title	
Collins, D. D.	Project Engineer	243
Bell, J. C., Jr.	Assistant Project Engineer, R & D Coordination	170
Roth, J.	Space Systems Engineering	82
Houmard, J. E.	Stress Analysis	72
Huber, J.	Microwave Engineering	42
Koller, W. B.	Microwave Engineering	78
Fretz, G.	Plastics Engineer	20
	Total	707*

*Total represents only those hours used by key personnel and does not include all hours expended on the program.

PART 8 - LIST OF REFERENCES

1. Jasik, Antenna Engineering Handbook, McGraw-Hill, N. Y., 1961.

2. Jacobsen and Ayre, Engineering Vibrations, McGraw-Hill, N. Y., 1958, p 163.

3. McComb, H. G., and Leonard, W., Slanted Drop Cords in Inflatable Airmat Beams, Journal of the Aerospace Sciences, Vol 29, pp 476 - 477, April 1962.

4. Timoshenko, S., and Wainowsky-Krieger, S., Theory of Plates and Shells, McGraw-Hill Book Company, 1959, pp 61 - 63.

Goodyear Aircraft Corp, Akron, Ohio. ON ADVANCED ANTENNA DESIGN TECHNIQUES by D. D. Collins and J. C. Bell Jr., GER 11045, Report No. 3, Third Quarterly Progress Report for Dec 62 - Mar 63. 95p incl. illus. (Contract DA-36-039 SC90746) DA Project No. 3A99-12-001. Unclassified Report An assessment of the particular needs of two broad categories of application (1) space vehicle antennas and (2) ground-based tracking antennas. Space system antenna concepts are sought for large-aperture appendage arrays and discrete radiators which will provide the best stowage to final dimension ratio, lowest possible weight, and lowest cost. Ground-based antenna system concepts are sought for large aperture collimators, large arrays, and sub-array elements of minimum weight and low cost, which can be simply and economically erected on site. The rigid-panel Swirlabola space antenna and the inflatable AIRMAT paraboloid and lenticular AIRMAT (over)	UNCLASSIFIED 1. Antennas - Design-development, reflectors, materials. 2. Antennas - Performance. 3. Antennas - Configuration, parabolic, Cassegrain. 4. Antennas, Reflectors, inflatable. I. Antenna Advanced Design Techniques - Space and Ground. II. Collins, D. D. and Bell, J. C. Jr. III. U.S. Army Electronics R&D Lab, Fort Monmouth, N. J. IV. Contract DA-36-039 SC-90746. UNCLASSIFIED

Goodyear Aircraft Corp, Akron, Ohio. ON ADVANCED ANTENNA DESIGN TECHNIQUES by D. D. Collins and J. C. Bell Jr., GER 11045, Report No. 3, Third Quarterly Progress Report for Dec 62 - Mar 63. 95p incl. illus. (Contract DA-36-039 SC90746) DA Project No. 3A99-12-001. Unclassified Report An assessment of the particular needs of two broad categories of application (1) space vehicle antennas and (2) ground-based tracking antennas. Space system antenna concepts are sought for large-aperture appendage arrays and discrete radiators which will provide the best stowage to final dimension ratio, lowest possible weight, and lowest cost. Ground-based antenna system concepts are sought for large aperture collimators, large arrays, and sub-array elements of minimum weight and low cost, which can be simply and economically erected on site. The rigid-panel Swirlabola space antenna and the inflatable AIRMAT paraboloid and lenticular AIRMAT (over)	UNCLASSIFIED 1. Antennas - Design-development, reflectors, materials. 2. Antennas - Performance. 3. Antennas - Configuration, parabolic, Cassegrain. 4. Antennas, Reflectors, inflatable. I. Antenna Advanced Design Techniques - Space and Ground. II. Collins, D. D. and Bell, J. C. Jr. III. U.S. Army Electronics R&D Lab, Fort Monmouth, N. J. IV. Contract DA-36-039 SC-90746. UNCLASSIFIED

Goodyear Aircraft Corp, Akron, Ohio. ON ADVANCED ANTENNA DESIGN TECHNIQUES by D. D. Collins and J. C. Bell Jr., GER 11045, Report No. 3, Third Quarterly Progress Report for Dec 62 - Mar 63. 95p incl. illus. (Contract DA-36-039 SC90746) DA Project No. 3A99-12-001. Unclassified Report An assessment of the particular needs of two broad categories of application (1) space vehicle antennas and (2) ground-based tracking antennas. Space system antenna concepts are sought for large-aperture appendage arrays and discrete radiators which will provide the best stowage to final dimension ratio, lowest possible weight, and lowest cost. Ground-based antenna system concepts are sought for large aperture collimators, large arrays, and sub-array elements of minimum weight and low cost, which can be simply and economically erected on site. The rigid-panel Swirlabola space antenna and the inflatable AIRMAT paraboloid and lenticular AIRMAT (over)	UNCLASSIFIED 1. Antennas - Design-development, reflectors, materials. 2. Antennas - Performance. 3. Antennas - Configuration, parabolic, Cassegrain. 4. Antennas, Reflectors, inflatable. I. Antenna Advanced Design Techniques - Space and Ground. II. Collins, D. D. and Bell, J. C. Jr. III. U.S. Army Electronics R&D Lab, Fort Monmouth, N. J. IV. Contract DA-36-039 SC-90746. UNCLASSIFIED

Goodyear Aircraft Corp, Akron, Ohio. ON ADVANCED ANTENNA DESIGN TECHNIQUES by D. D. Collins and J. C. Bell Jr., GER 11045, Report No. 3, Third Quarterly Progress Report for Dec 62 - Mar 63. 95p incl. illus. (Contract DA-36-039 SC90746) DA Project No. 3A99-12-001. Unclassified Report An assessment of the particular needs of two broad categories of application (1) space vehicle antennas and (2) ground-based tracking antennas. Space system antenna concepts are sought for large-aperture appendage arrays and discrete radiators which will provide the best stowage to final dimension ratio, lowest possible weight, and lowest cost. Ground-based antenna system concepts are sought for large aperture collimators, large arrays, and sub-array elements of minimum weight and low cost, which can be simply and economically erected on site. The rigid-panel Swirlabola space antenna and the inflatable AIRMAT paraboloid and lenticular AIRMAT (over)	UNCLASSIFIED 1. Antennas - Design-development, reflectors, materials. 2. Antennas - Performance. 3. Antennas - Configuration, parabolic, Cassegrain. 4. Antennas, Reflectors, inflatable. I. Antenna Advanced Design Techniques - Space and Ground. II. Collins, D. D. and Bell, J. C. Jr. III. U.S. Army Electronics R&D Lab, Fort Monmouth, N. J. IV. Contract DA-36-039 SC-90746. UNCLASSIFIED

ground-based antennas, selected during second quarter evaluation, are analyzed further. Electrical, structural, and mechanical design considerations are discussed. Swirlabola size is 10 feet in diameter with f/D of 0.35. Analysis shows thermal and dynamic deflection within required range for Swirlabola. Design configuration for 40-foot-diameter ground-based AIRMAT antennas presented. Analysis of Cassegrain feed blockage indicates no significant problems. Structural analysis indicates deflections within required limits. For the lenticular antenna phase delay due to AIRMAT, drop cords may limit use below 5000 mc. Preliminary tests of flexible foam reflector material are shown. Preliminary section model indicates radial fabric web construction feasible for models.

UNCLASSIFIED

UNCLASSIFIED

ground-based antennas, selected during second quarter evaluation, are analyzed further. Electrical, structural, and mechanical design considerations are discussed. Swirlabola size is 10 feet in diameter with f/D of 0.35. Analysis shows thermal and dynamic deflection within required range for Swirlabola. Design configuration for 40-foot-diameter ground-based AIRMAT antennas presented. Analysis of Cassegrain feed blockage indicates no significant problems. Structural analysis indicates deflections within required limits. For the lenticular antenna phase delay due to AIRMAT, drop cords may limit use below 5000 mc. Preliminary tests of flexible foam reflector material are shown. Preliminary section model indicates radial fabric web construction feasible for models.

UNCLASSIFIED

UNCLASSIFIED

ground-based antennas, selected during second quarter evaluation, are analyzed further. Electrical, structural, and mechanical design considerations are discussed. Swirlabola size is 10 feet in diameter with f/D of 0.35. Analysis shows thermal and dynamic deflection within required range for Swirlabola. Design configuration for 40-foot-diameter ground-based AIRMAT antennas presented. Analysis of Cassegrain feed blockage indicates no significant problems. Structural analysis indicates deflections within required limits. For the lenticular antenna phase delay due to AIRMAT, drop cords may limit use below 5000 mc. Preliminary tests of flexible foam reflector material are shown. Preliminary section model indicates radial fabric web construction feasible for models.

UNCLASSIFIED

UNCLASSIFIED

ground-based antennas, selected during second quarter evaluation, are analyzed further. Electrical, structural, and mechanical design considerations are discussed. Swirlabola size is 10 feet in diameter with f/D of 0.35. Analysis shows thermal and dynamic deflection within required range for Swirlabola. Design configuration for 40-foot-diameter ground-based AIRMAT antennas presented. Analysis of Cassegrain feed blockage indicates no significant problems. Structural analysis indicates deflections within required limits. For the lenticular antenna phase delay due to AIRMAT, drop cords may limit use below 5000 mc. Preliminary tests of flexible foam reflector material are shown. Preliminary section model indicates radial fabric web construction feasible for models.

UNCLASSIFIED

DISTRIBUTION LIST

Address	Copy No.
Chief of Research and Development OCS, Department of the Army Washington 25, DC	1
Commanding General US Army Electronics Command ATTN: AMSEL-AD Fort Monmouth, New Jersey	2-4
Director, US Naval Research Laboratory ATTN: Code 2027 Washington 25, DC	5
Commanding Officer and Director US Navy Electronics Laboratory San Diego 52, California	6
Headquarters, Electronic Systems Division ATTN: ESRR & ESSD L. G. Hanscom Field Bedford, Massachusetts	7-8
Commander, Armed Services Technical Information Agency ATTN: TIPCR Arlington Hall Station Arlington 12, Virginia	9-12
Commanding Officer US Army Electronics Research and Development Laboratory ATTN: Director of Research/Engineering Fort Monmouth, New Jersey	13
Commanding Officer US Army Electronics Research and Development Laboratory ATTN: Technical Documents Center Fort Monmouth, New Jersey	14

DISTRIBUTION LIST (Continued)

Address	Copy No.
Missiles and Space Division Lockheed Aircraft Corporation ATTN: Technical Information Center 3251 Hanover Street Palo Alto, California	15
Fairchild Stratos Corporation ATTN: Librarian Hagerstown, Maryland	16
National Aeronautics and Space Administration Spacecraft Systems and Projects Division ATTN: Mr A. Kampinsky, Code 621 Goddard Space Flight Center Greenbelt, Maryland	17
Commanding General US Army Satellite Communications Agency ATTN: AMXSC-5 Fort Monmouth, New Jersey	18-19
Commanding Officer US Army Electronics Research and Development Laboratory ATTN: SELRA/NRA (Mr. F.J. Triolo) Fort Monmouth, New Jersey	20-21
General Electric Company Ordnance Department ATTN: Mr. Paul Blasangame Pittsfield, Massachusetts	22
Commanding Officer US Army Electronics Research and Development Laboratory ATTN: SELRA/LNR (Marine Corps Liaison Office) Fort Monmouth, New Jersey	23